ABSTRACT

Title of Thesis:	DETERMINING STRENGTH CAPACITY OF DETERIORATED REINFORCED CONCRETE BRIDGE SUBSTRUCTURES

Timothy K. Saad, Master of Science, 2010

Thesis directed by: Research Professor, Doctor Chung C. Fu
Department of Civil and Environmental Engineering

Corrosion of steel reinforcement is a major factor in the deterioration of highway and bridge infrastructure. Knowing the initiation time of corrosion on a reinforced concrete structure provides a much needed source of information in evaluating the service life of the structure. To find the corrosion initiation time the effects of carbonation and chloride are examined. Furthermore, the different variables that affect the ingress of carbonation and chloride are also examined and analyzed together. Probabilistic modeling and stochastic design of these variables will determine the initiation of corrosion, the amount of corrosion, and the strength loss of the concrete pier. This process will help classify deteriorating structure into the National Bridge Inventory (NBI) condition ratings from the Federal Highway Administration.

DETERMINING STRENGTH CAPACITY OF DETERIORATED
REINFORCED CONCRETE BRIDGE SUBSTRUCTURES

by

Timothy Kenneth Saad

Thesis submitted to the Faculty of the Graduate School of the

University of Maryland, College Park in partial fulfillment

of the requirements for the degree of

Master of Science

2010

Advisory Committee:
      Professor Chung C. Fu, Chair
      Professor Amde M. Amde
      Professor Sherif M. Aggour

1. Table of Contents

Table of Figures

1. Introduction

1.1 Background

A considerable percentage of highway bridges in North America are in a structurally/functionally deficient state due to aging, aggressive environments, and increased traffic load and volume. In 2008, about ¼ bridges in America were either structurally deficient or functionally obsolete. On a bridge structure, the substructure is one of the most vulnerable components to the routine application of deicing salts, repeated freeze-thaw cycles, and other damaging effects including environmental effects. Nevertheless, these deteriorating effects demand proper maintenance, repair and replacement techniques. Two questions must always be answered before a substructure undergoes possible rehabilitation:

(1) How can the condition of the substructure be assessed?

(2) Based on the assessment, can the bridge substructure unit be rehabilitated or must it be replaced?

Having accurate assessment information is essential, due to the high cost associated with replacing every bridge components.

1.2 Problem Statement

Reinforced concrete structures have proven to be vulnerable to the damaging effects of carbonation and chlorides which are born from seawater and deicing salts. The deterioration of concrete structures due to chloride-induced reinforcement corrosion is one of the largest contributing factors affecting the strength capacity of concrete piers. In a reinforced concrete structure, the concrete cover around the reinforcement provides protection to the reinforcement from environmental damaging effects. The corrosion of the steel reinforcement leads to concrete fracture through cracking and spalling of the concrete cover and most importantly a reduction in the concrete and reinforcement cross sections. As a result of the corrosion, the reinforced

concrete pier experiences reduction in its strength and ductility, and this reduces the safety, serviceability and life of the concrete structure.

The objective of this study was to develop a generalized model that exemplifies the current condition or strength of concrete substructures that have experienced degradation: the decrease in performance over time. The two main factors of carbonation and chloride have the largest effect on the load-bearing capacity of concrete structures. The prediction of the performance and of the strength concrete structures, subjected to carbonation and chlorides, requires a thorough understanding of the ingress of carbonation and chloride in the concrete, the corrosion initiation within the reinforcement, and the damage of the concrete.

This thesis investigates and examines the degradation of concrete piers through research and data collected from other researches in order to find the most reliable calculation. Uncertainties in the problems will be addressed and probabilistic modeling and stochastic design methods are used for the calculation of uncertainties. Essentially, the models will also help to determine the service life of the substructure. The service life is best described as the time at which the strength of the reinforced concrete pier is reduced beyond the point which the structure is no longer reliable. As discussed later, the service life is considered to be equal to the sum of the initiation and the propagation time.

1.3 Service Life Modeling

The service life of a structure is the period of time in which it is able to comply with the given requirements of safety, stability, serviceability and function, without requiring extraordinary costs of maintenance and repair. Modeling the durability of reinforced concrete structures requires a quantitative understanding of the structures environment, transport methods of deteriorating factors, the corrosion process, and a quantitative assessment of concrete design.

As best defined by the National Cooperative Highway Research Program (NCHRP) (Sohanghpurwala, 2006), the process of chloride induced corrosion of steel in concrete is described in the following numerical stages:

1. Chlorides in the environment build up on the concrete surface.
2. Chlorides are transported through the concrete mainly through the diffusion process.
3. The chloride concentration builds up with time at the steel surface.
4. Once the chloride level achieves a critical threshold level, the protective oxide layer on the steel breaks down and corrosion starts.
5. Corrosion creates rust on the steel, which creates a larger volume of products that exert tensile stresses on the concrete.
6. Concrete is weak in tension, so the concrete cracks either vertically to the surface or horizontally to form a Delamination between reinforcing bars.
7. Cracks form pot holes or spalls, which lead to a degradation in the structure's appearance, function, and safety, leading to end of service life or time to repair.
8. The repairs may be made, and the cycle continues in the undamaged areas and in the repaired areas.

Therefore, some of the more important variables in the process of corrosion modeling are:

- Determining the chloride ion content at the surface of the concrete, C_s
- Calculating the rate of transport from the surface of the concrete to the reinforcing steel, aka the chloride diffusion coefficient, D
- Determining the chloride threshold amount that the chloride surpasses to initiate corrosion, C_{th}
- Estimating the time the chlorides reach the reinforcing steel, initiation period, T_i
- Estimating the time from corrosion initiation to first cracking, propagation period, T_p
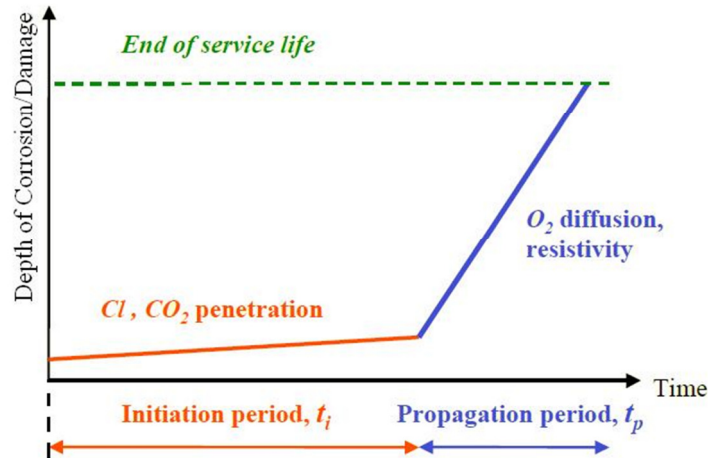
Figure 1.1 Deterioration Model of Reinforced Concrete
(Life-365)

Many proposed service life models have followed the simplified approach seen in Figure 1.1. In

accordance with the process of chloride induction set forth in the National Cooperative Highway

Research Program numerical stages (described above), the initiation period is exemplified in

stages 1 through 4 as the chloride penetrates toward the reinforcement and the propagation

period is exemplified in stages 5 through 7 until cracks become visible at the concrete surface.

The time to the end of service life is reached at the end of the propagation period when an

unacceptable amount of damage is reached.

The Federal Highway Administration currently uses the model found in Figure 1.2 to represent

the maintenance-free life of a structure. In this model, the propagation period is split up into the

cracking of the external concrete, T_c, and the time for the surface cracks to evolve into spalls, T_s.

According to the Federal Highway Administration, a structure will be in need of maintenance at

the end of its maintenance-free service life, T_{mf}. The maintenance-free service life does not

include the occasional minor or routine repairs made during the life of the structure. While

researches tend to agree on the parameters of the service life model, there is not currently a

workable mathematical model that makes the service life model a proper design procedure for
service life estimations.
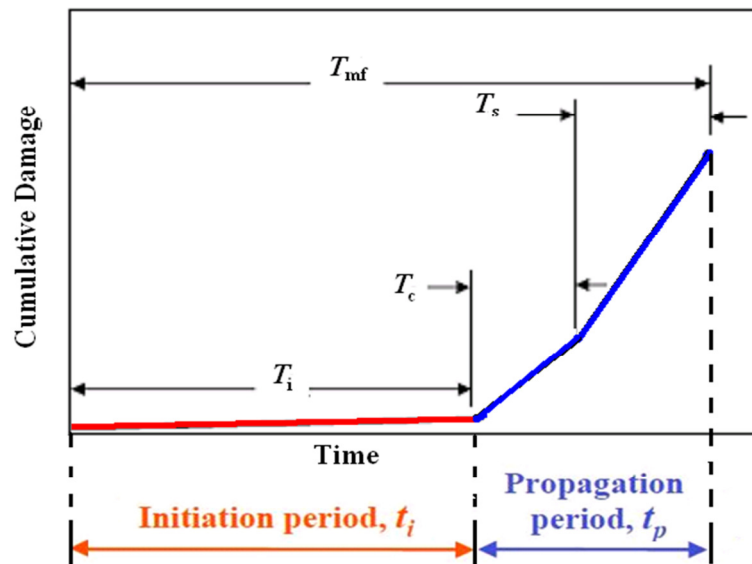
Figure 1.2   Steps of Reinforced Concrete Deterioration due to Chloride-Induced Corrosion
(Federal Highway Administration)

1.3.1 Initiation Period

The initiation period can be described as the time it takes for the chlorides to penetrate the

concrete cover depth until the reinforcement is reached, but still leaving the reinforcement in a

passive state. The initiation time is best treated as a stochastic variable due to the varying effects

of the distribution of chloride on the concrete surface, the different positions of reinforcement,

and the various mixtures of concrete.

During the penetration of chlorides in the concrete, the chlorides continuously accumulate over

time until they reach an amount of chloride that is considered an unacceptable amount at the

reinforcement level. This amount of chloride is known as the threshold amount. From this

information, the corrosion initiation time is dependent on several parameters, including the

concrete cover depth, surface chloride concentration, concrete cover, various components of a

concrete mix, and the chloride threshold. Thus, the corrosion initiation period is best referred to as the time during which chlorides penetrate the concrete and the reinforcement begins corroding.

1.3.2 Propagation Period

The propagation period is initiated upon reaching the chloride threshold amount. This propagation period begins with the onset of the corrosion process. Corrosion begins once the passivation of steel is destroyed and the reinforcement starts corroding actively. Active corrosion of the steel causes a large production of rust products and causes the concrete to detach from the steel and eventually crack. It is the cracking of the concrete that demonstrates a significant strength reduction of the reinforcement and the structure in general, and the structure is at the verge of its estimated end of service life.

1.3.3 Time to Damage

Time to damage (T_d) is the sum total of the initiation time period (T_i) and the propagation time period (T_p). Therefore, the time to damage is the time required for chloride to diffuse down to the steel depth, surpass the corrosion threshold, corrode the reinforcement, and produce cracking and/or spalling of the concrete (Sohanghpurwala 2006).

$$T_d = T_i + T_p \qquad \text{Equation 1-1}$$

1.4 Maryland Test Procedures

The following testing procedures are conducted by the state of Maryland. These procedures were compiled by a previous research team at the University of Maryland (Howlader 2008) who investigated the state of Maryland's routinely conducted lab and field tests on concrete structures.

1.4.1 Visual Inspection

Inspections are generally started with visual observations of the concrete substructure based on visible signs of distress such as cracking, delamination, or spalling (as seen in Figure 1.3).

a) Surface cracking   b) Delamination   c) Spalling
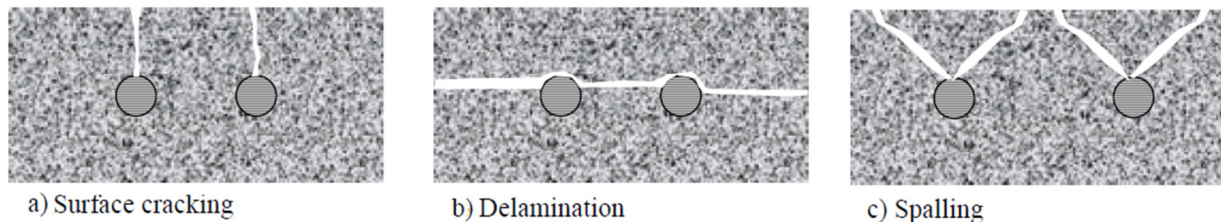
Figure 1.3   Schematic Presentation of Cracking Failure (Lounis and Daigle, 2008)

While visual inspection is not enough to determine the need and methodology of repair, it is a preliminary screening process that helps determine the types of nondestructive and laboratory tests to undergo for gathering more information used in decision making. Visual inspection should be supported with photographs to represent the current damage.

1.4.2 Drilling a Core

AASHTO T-24 or ASTM C42

In accordance with the American Society for Testing and Materials (standard C42), concrete core specimens are obtained when more information is needed about the in-place concrete quality or when there are signs of distress in the structure. In general, concrete strength is affected by the location of the concrete in the structure, with concrete at the base stronger than the concrete at the top. The strength of concrete measured from the concrete cores is affected by the amount and distribution of moisture in the specimen. While a concrete core specimen may not give the identical moisture condition of the concrete in the structure, this test method is intended to provide replicable moisture conditions to laboratory variations and to reduce the effects of moisture introduced during concrete preparation.   Nonetheless, Maryland primarily uses the core

sampling as a way to determine the depth of deterioration and cracking of concrete. The amount of the core samples are determined from results from the visual inspection and corrosion surveys.

The diameters of the cores should be as large as possible to ensure that the local effects of the aggregates do not adversely affect the results. In the United States, typical core diameters are found at 1", 2", 3". A water cooled diamond-tipped overcoring drill bit is used to extract the concrete specimen. This process should be done with caution to ensure no contact between the drill bit and the steel reinforcement.

1.4.3 Using a Covermeter

The covermeter is used to find the exact location of the rebar in the concrete and orientation of the rebar. Maryland uses a Pachometer device in order to carry out this measurement and determine the concrete cover thickness. While, Maryland uses the results of a covermeter test to provide additional information for structures proposed for rehabilitation, the results are not necessarily used for acceptance or rejection of the proposed repairs or rehabilitation.

1.4.4 Half-Cell Potential

Half-cell potential mapping has been a shown to be a powerful and effective non-destructive technique both in condition assessment and in repair of reinforced concrete structures. Under the same procedure, half-cell potential measurements can be performed on new and existing concrete structures. The half-cell potential measurement is an electrochemical technique that shows presence and severity of corrosion. When an electrical connection is made on the reinforcement, an external reference electrode is passed over the concrete and the potential voltage difference is recorded. Depending on the chloride content, cover thickness, water/cement ratio and temperature, different potential values indicate corrosion of the

reinforcement among various structures. Combined with the tests of the covermeter, a fairly accurate assessment of corrosion in the reinforced concrete structure can be made.

The following guidelines (Table 1.1) have been developed for evaluating the corrosion potentials performed with a copper-copper sulfate (Cu-CuSO$_4$) half cell. These guidelines can be found in American Society for Testing and Materials ASTM C-876 (Sohnaghpurwala 2006).

- A good understanding of a half-cell potential measurement is that a 90% probability of no corrosion activity on the reinforcing bar at the time of measurement exists if the half-cell potential is less negative than -0.200 V.
- An increasing probability of corrosion activity exists if the half-cell potential falls between −0.200 V and -0.350 V. This probability depends on factors such as chloride content at the reinforcing bar level, moisture content of the concrete, temperature, etc. Typically, values within this range are said to have an uncertain probability of corrosion activity.
- A 90% probability of corrosion activity on the reinforcing bar at the time of measurement exists if the half-cell potentials are more negative than -0.350 V.

Half- cell potential reading	Corrosion activity
less negative than -0.200 V	90% probability of no corrosion, Low Risk
between -0.200 V and -0.350 V	an increasing probability of corrosion, Intermediate Risk
more negative than -0.350 V	90% probability of corrosion, High Risk
more negative than -0.500 V	severe corrosion, corrosion induced cracking may occur

Table 1.1 ASTM Interpretation of Half-Cell Potential Readings

2. Classification

2.1 Evaluation of Concrete Piers

As we know, reinforced concrete substructures are originally designed to resist a certain amount of load. Once a reinforced concrete substructure begins to experience any type of corrosion or deterioration, the substructure loses some of its strength. Therefore, it is important to evaluate damaged substructures and find out the substructure's percentage capacity loss and to make sure the substructure is still capable of resisting the amount of load necessary. Depending on the amount of deterioration the substructure is categorized into ten condition ratings which were developed by the FHWA National Bridge Inspection Standards and are a part of the Maryland State Highway Administration annual bridge inspection program. These ratings, numbered from 0 to 9, are based on on-site inspections of each bridge structure/substructure and highly consider the structures age and the environmental conditions the structure has been subjected to. When evaluating the reinforced concrete structure, Table 2.1 lists the ratings with their appropriate condition descriptions.

Rating	Condition Description
9	Excellent condition
8	Very good condition – no problems noted
7	Good condition – some minor problems
6	Satisfactory condition – structural elements show some minor deterioration
5	Fair condition – all primary structural elements are sound, but may have minor section loss, racking, spalling or scour
4	Poor condition – advanced section loss, deterioration, spalling or scour
3	Serious condition – loss of section, deterioration, spalling or scour have seriously affected primary structural components. Local failures are possible. Fatigue cracks in steel or shear cracks in concrete may be present.
2	Critical condition – advanced deterioration of primary structural elements. Fatigue cracks in steel or shear cracks in concrete may be present or scour may have removed substructure support. Unless closely monitored, it may be necessary to close the bridge until corrective action is taken.
1	"Imminent" failure condition – major deterioration or section loss present in critical structural components or obvious vertical or horizontal movement affecting structure stability. Bridge is closed to traffic but corrective action may put back in light service
0	Failed condition – out of service – beyond corrective action

Table 2.1   Substructure Condition Rating by the FHWA National Bridge Inspection Standards

Furthermore, the ratings can then determine if the structure can be left alone or if the structure would need further analysis or the immediate action of replacement or rehabilitation. Actions associated with their respective condition ratings are listed in Table 2.2.

Rating	Condition Description	Action
9	Excellent condition	No Action
8	Very good condition	
7	Good condition	
6	Satisfactory condition	
5	Fair condition	Clarify rating
4	Poor condition	
3	Serious condition	
2	Critical condition	
1	"Imminent" failure condition	Immediate Action
0	Failed condition	

Table 2.2   Actions associated with Condition Rating Classification

In order to classify the concrete substructures into these condition ratings, the substructures undergo visual observations, computer program analyses, chloride diffusion spreadsheets, and possibly field surveys. The flowchart in Figure 2.1 represents a decision tree that helps determining the current condition or the strength of the substructure.

As seen in the first stage of the flowchart, if the structure is thought to be in satisfactory condition or better (ratings = 6, 7, 8, 9), the decision of "No Action" can be made right from the start. Likewise, if the structure is thought to be rated into failure or failed condition (rating = 1, 0), then the structure inarguably needs to be replaced.

A structure that is decided to be of fair condition (rating = 5) is only analyzed through the Life 365 program and coordinated with a Chloride Diffusion Chart. A structure within the critical condition and poor condition categories (ratings 2 – 4) must undergo a different logic procedure for further analysis in order to determine whether the structure falls into the replacement or rehabilitation category. This further analysis accounts for the necessity of a field test. If a field

11

test is determined to be necessary, the structure would undergo corrosion surveys, chloride surveys, and boring surveys. However, if they do not undergo a field test, they are treated similarly to a structure with that is categorized as being in "Fair condition" (rating = 5).
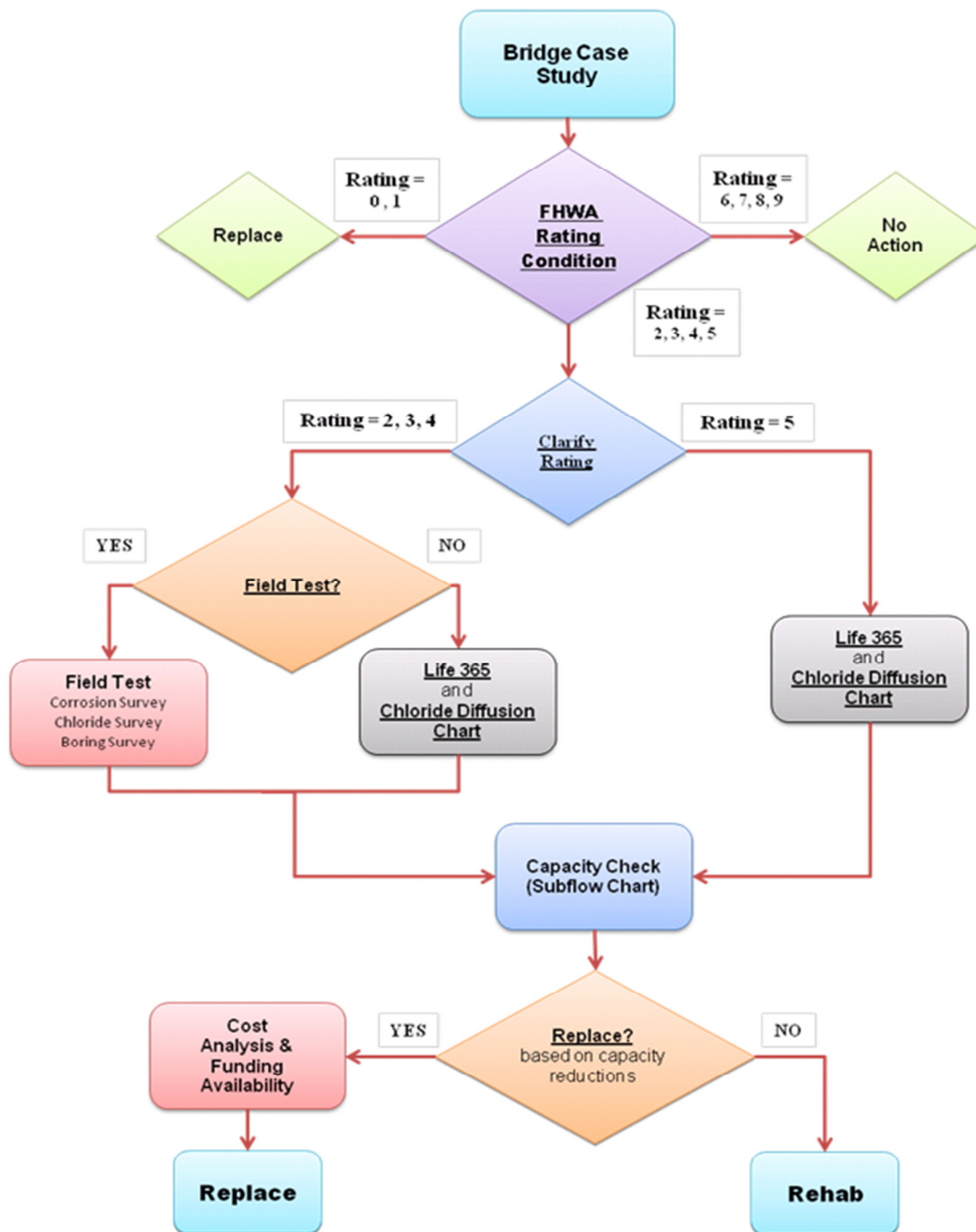
Figure 2.1   Decision Tree for Determining current Condition of Substructure

2.2 Determining Structural Capacity (Sub-flow Chart)

The field test results from structures within the ratings 2-5 are further analyzed for determining the amount of strength left in the structure. Information about the structure is compiled into a new sequential diagram or a sub-flowchart (Figure 2.2), which derives the answer for the amount reduction in R/C capacity and the final answer of rehabilitating or replacing the structure. Therefore, concrete substructures can be examined in accordance with their materials and properties, which will help determine the intensities or extents of their damage as well as predict the future deterioration or ongoing corrosion in the structure.
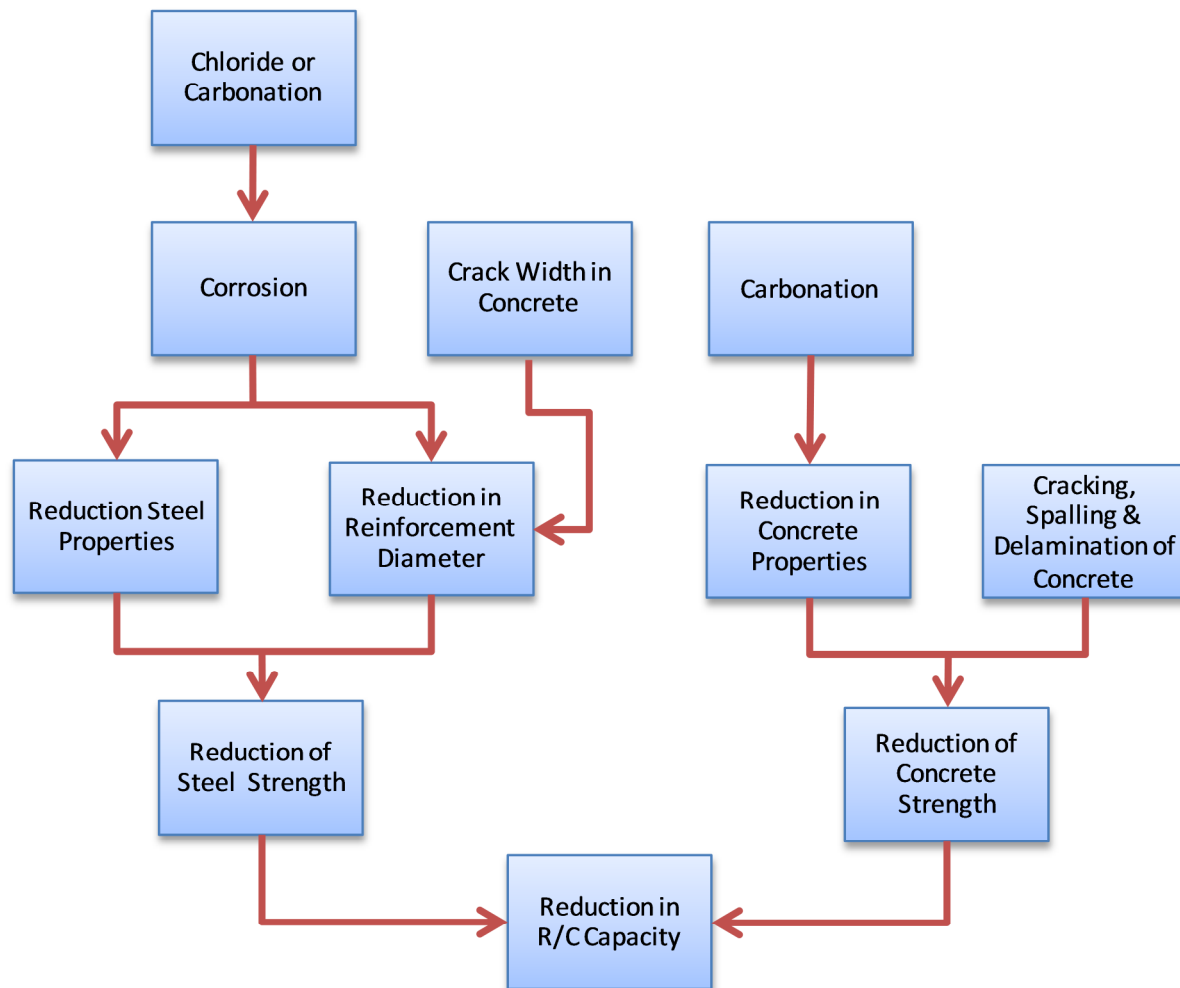
Figure 2.2   Sub-Flowchart for the Amount Reduction in R/C Capacity

3. Principles and Methods of Design

The reliability is defined in structural engineering as the ability of the structure to fulfill its design purpose. The structure must fulfill performance requirements, while surviving environmental conditions. Performance of a structure is defined as the behavior of the structure and is related to the structure's load bearing capacity, stability, or safety. The performance of the structure is a function of time, thus the structures are often described as "over time" or "with time." (Sarja et al. 1996). If all the performance requirements are filled, a structure will remain in its service life period. Therefore, the reliability of a structure can be assessed by the probability of meeting satisfactory performance requirements within a stated time period (Ayyub 2003).

If the end of service life is defined as the period where the structure needs maintenance or repair of components, then it is important to find the maximum probability of keeping the structure from reaching its service life, i.e. probability of failure. Failure occurs if the resistance of loading the structure can withstand is smaller than the applied loads (Figure 3.1).

$$\{failure\} = \{R < S\} \hspace{3cm} \text{Equation 3-1}$$
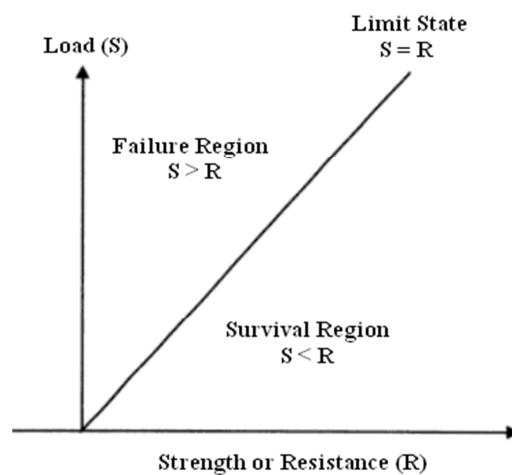
Figure 3.1   Performance Function for a Linear Two-Random Variable Case

Figure 3.2 illustrates the relationship between the performance function, the loading distribution ad the resistance distribution. As seen in the figure, when Z < 0, the function is in the failure state. And the probability of failure is defined as

$$P_f = P\{R < S\}$$ Equation 3-2

Resistance of structure, R
Loading applied to structure, S

Failure probability is also a function of time and should be written as,

$$P_f(t) = P\{R(t) < S(t)\}$$ Equation 3-3
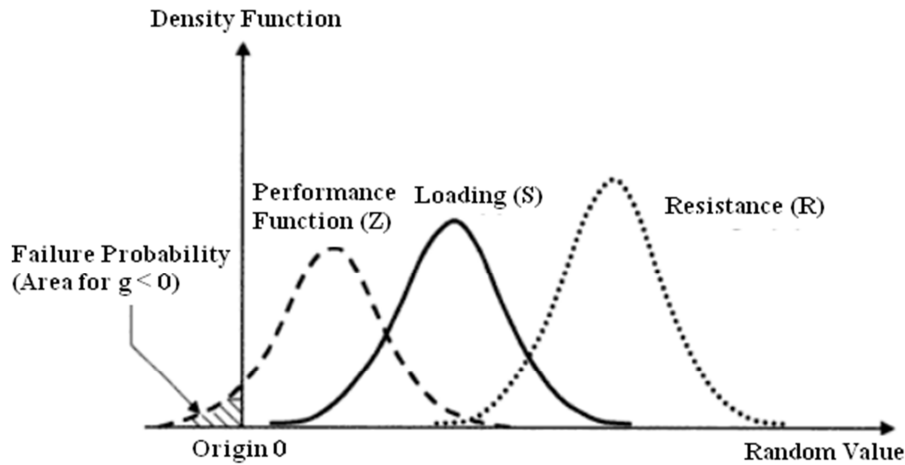
Figure 3.2 Performance Function for Reliability Assessment (Ayyub 2003).

3.1 Deterministic Design vs. Stochastic Design

In deterministic durability design, the distributions of load, resistance, and service life are used as deterministic quantities. These quantities are chosen by selecting an appropriate combination of values for design parameters. Accordingly, the design formula is written as,

$$R(t_g) - S(t_g) > 0$$ Equation 3-4

t_g = target service life

In stochastic durability design, the distributions of load, resistance, and service life are expressed as the probability that the design formula is not true. The design formula is written similarly to

15

the deterministic with the addition of maximum allowable failure probability included to the

final condition,

$$P\{failure\}_{t_g} = P\{R - S < 0\}_{t_g} < P_{fmax} \qquad \text{Equation 3-5}$$

P{failure}$_{tg}$ = probability of failure of the structure with t$_g$
P$_{fmax}$ = maximum allowable failure probability

In order to solve Equation 3-5 the distributions of load and resistance are solved for. When the

resistance, R, and the load, S, are normally distributed performance functions, the failure

probability can be determined using the reliability index, β. The reliability index for

uncorrelated random variables is given by,

$$\beta(t) = \frac{\mu_R - \mu_S}{\sqrt{\sigma_R^2 - \sigma_S^2}} = \frac{\mu[R,t] - \mu[S,t]}{\sqrt{\sigma^2[R,t] - \sigma^2[S,t]}} \qquad \text{Equation 3-6}$$

μ = mean value
σ = standard deviation
β is normally distributed $(\mu, \sigma) \rightarrow (0, 1)$

With the assumption of normal distribution, then the failure probability P$_f$ can be shown as,

$$P_f = 1 - \Phi(\beta) \qquad \text{Equation 3-7}$$

where Φ is the cumulative distribution function of the standard normal variation.

3.2 Initiation Period with Log-Normal Distribution

Service life models often show a strong incline towards short service lives. The probability

density function also peaks rapidly before decreasing slowly to an infinite service life. The best

fitting model to represent this distribution is a log-normal model, which means the service life is

distributed normally on a logarithmic time scale.

A log-normal curve is used to model the time to initiation of corrosion (initiation period) for both

carbonation and chloride. Both of these deteriorating factors ingress through the concrete cover

and cause corrosion on the surface of the concrete. The initiation time of corrosion, t_{cr}, occurs

when the reinforcement initiates corrosion or at the end of the initiation period t_i. Therefore, no

corrosion takes place when the cover depth is greater than the depth of the carbonation or

chlorides.

$$C(c,t_{in}) < C_{th} \quad \text{implies "no corrosion"}$$
$$C(c,t_{in}) = C_{th} \quad \text{implies "initiating corrosion"}$$
$$C(c,t_{in}) > C_{th} \quad \text{implies "ongoing corrosion"}$$

Under constant diffusivity, the corrosion initiation time is

$$t_{cr} = \left(\frac{c}{k_1}\right)^2 \qquad\qquad \text{Equation 3-8}$$

c = concrete cover depth, mm

k_1 = first year ingress, $mm/\sqrt{year}$

The probability of failure for carbonation and chloride ingress can be written as,

$$P_f(corrosion) = P\{k(t) < c(t)\} \qquad\qquad \text{Equation 3-9}$$

The probability density function of a lognormal distribution is found from:

$$f_x(x) = \frac{1}{x\sigma_Y\sqrt{2\pi}} \exp\left[-\frac{1}{2}\left(\frac{\ln x - \mu_Y}{\sigma_Y}\right)^2\right] \text{ for } 0 < x < \infty \qquad \text{Equation 3-10}$$

It is normal to use the notation $X \sim LN(\mu_Y, \sigma_Y^2)$ to provide an abbreviated description of the

lognormal destruction. This notation shows that X is log-normally distributed with the

parameters, μ_Y and σ_Y^2.

In a lognormal distribution μ_X and σ_X^2 are not equal to the parameters of the distribution, μ_Y and σ_Y^2.

Instead, μ_X and σ_X^2 are the parameters on a normal distribution and must be converted to a lognormal

distribution. This relationship can be solved for when the expected mean and coefficient of variation

are known.

17

Cornell's method of reliability index is good to use in stochastic design because it takes some knowledge of the stochastic distribution into account: the expectation value and the standard deviation of the governing parameters (Poulsen, 2006).

The expectation value for a log-normal curve,

$$\mu_X = E[T_{cr}] = \left(\frac{\mu_c}{\mu_k}\right)^2 (1 + V_c^2)(1 + V_k^2)^3 \qquad \text{Equation 3-11}$$

μ_c = mean value, cover depth
μ_k = mean value, ingress rate
V_c = coefficient of variation, cover depth
V_k = coefficient of variation, ingress rate

Coefficient of variation is given by

$$V[T_{cr}] = \sqrt{(\{1 + V_c^2\}\{1 + V_k^2\})^4 - 1} \qquad \text{Equation 3-12}$$

Also written as,

$$\sigma_X = S[T_{cr}] = E[T_{cr}] \times V[T_{cr}] \qquad \text{Equation 3-13}$$

The parameters curve, μ_γ and σ_γ, of a lognormal distribution can be found if the values of the mean E[x] and V[x] are known:

$$\sigma_\gamma^2 = \ln\left[1 + \left(\frac{\sigma_X}{\mu_X}\right)^2\right] \qquad \text{Equation 3-14}$$

$$\mu_\gamma = \ln(\mu_X) - \frac{1}{2}\sigma_\gamma^2 \quad \rightarrow \quad \mu_\gamma = \ln(E[T_{cr}]) - \frac{1}{2}\ln\left[1 + \left(\frac{S[T_{cr}]}{E[T_{cr}]}\right)^2\right] \qquad \text{Equation 3-15}$$

3.3 Characteristic Initiation Period of Time

Taking into account the two parameters, concrete cover and ingress of carbonation or chlorides, the probability density function can be graphically and numerically modeled. The characteristic value of the initiation time, K[T$_{cr}$] can also be found and used to strengthen the results. The

18

lower characteristic value is defined as the 5% quantile and the upper defined as the 95% quantile. This characteristic value gives the value below which the chosen percentage of all chloride profiles with the input variables are expected to fall. In design, it is generally only the lower characteristic value that is of interest.

The characteristic value of the initiation time is written as,

$$K[T_{cr}] = \exp(E[\ln T_{cr}] - (1.65)S[\ln T_{cr}])$$
Equation 3-16

Mean value of the logarithm of the initiation period of time (when assuming constant chloride diffusivity and a log normal distribution)

$$E[\ln T_{cr}] = \ln\left\{\frac{(1+V_k^2)\,\mu_c^2}{(1+V_c^2)\,\mu_k^2}\right\}$$
Equation 3-17

For the concrete cover of the reinforcing bars

$$\mu_c = E[C] \qquad\qquad \sigma_c = S[C] \qquad\qquad V_c = \sigma_c/\mu_c$$

Standard Deviation of the logarithm of the initiation period of time is

$$S[\ln T_{cr}] = 2\sqrt{\ln(\{1 + V_c^2\}\{1 + V_k^2\})}$$
Equation 3-18

Inserting the mean value and standard deviation into the characteristic of initiation time equation

$$K[T_{cr}] = \frac{(1+V_k^2)\,\mu_c^2}{(1+V_c^2)\,\mu_k^2} \exp\left(-3.3\sqrt{\ln(\{1 + V_c^2\}\{1 + V_k^2\})}\right)$$
Equation 3-19

4. Carbonation Induced Corrosion

Carbonation refers to the dissolving of carbon dioxide (CO_2) through the pores of concrete. The carbon dioxide can then lower the alkalinity of the concrete to a pH value below pH 9 in the carbonated zone, where concrete typically has a pH value larger than 11 (Parameswaran, et al. 2008). The good news about the change in pH values means that carbonation can be tested through a carbonation survey. However, carbonation of concrete can lead to corrosion of reinforcement. Time to initiate corrosion is a function of deterioration rate, which depends on the thickness and permeability of concrete cover, density, w/c (water cement ratio) and environmental affects. From this information we can tabularize the different categories the different classes of carbonization in Table 4.1Classes of carbonation based on the carbonation depth.

Depth of Carbonization	1	Ratio of Carbonation depth/cover thickness << 1
	2	Ratio of Carbonation depth/cover thickness < 1
	3	Ratio of Carbonation depth/cover thickness = 1
	4	Ratio of Carbonation depth/cover thickness > 1
	5	Ratio of Carbonation depth/cover thickness >> 1

Table 4.1   Classes of carbonation based on the carbonation depth

As defined, the service life of a structures the period of time during which the performance of the structure is kept at a level compatible with the fulfillment of performance requirements, provided it is properly maintained. Carbonation will begin cracking on the concrete structure, once carbonation reaches the front of the rebar (initiation time for corrosion t_0) plus the time required for the rust to build up and split the cover (propagation period, t_1). In carbonated concrete at high humidity levels, the corrosion rates are high and so the arrival of carbonation at the rebar is shortly followed by the splitting of concrete cover. Therefore, under the consideration of carbonation, the time for initiation of corrosion can be considered a good approximation of the

service life of concrete. The deterioration rate of concrete cover due to carbonation is expressed

mathematically as,

$$\mu(d) = k_c t^{1/2} \quad \rightarrow \quad t_1 = \left(\frac{c}{k_c}\right)^2 \qquad\qquad \text{Equation 4-1}$$

$\mu(d)$= the mean of the depth of carbonation (mm)
k_c= the carbonation ingress rate (mm/√[year])
t= time (years)

$$k_c = c_{env}\, c_{air}\, a(f_{ck}+8)^b \qquad\qquad \text{Equation 4-2}$$

f_{ck}=the characteristic cubic compressive strength of concrete (typically 4000psi or 30 MPa)

c_{env} =the environmental coefficient, (MPa)	
Structures Sheltered from rain	*1.0*
Structures Exposed to Rain	*0.5*

c_{air} =the coefficient of air content, (MPa)	
1.0	Non-air-entrained
0.7	Air-entrained

Binding Agent	a	b
Portland Cement Binder (Type 1)	*1800*	*-1.7*
PC +28% Fly Ash (Type 2)	*360*	*-1.2*
PC +70% blast furnace slag (Type 2)	*360*	*-1.2*
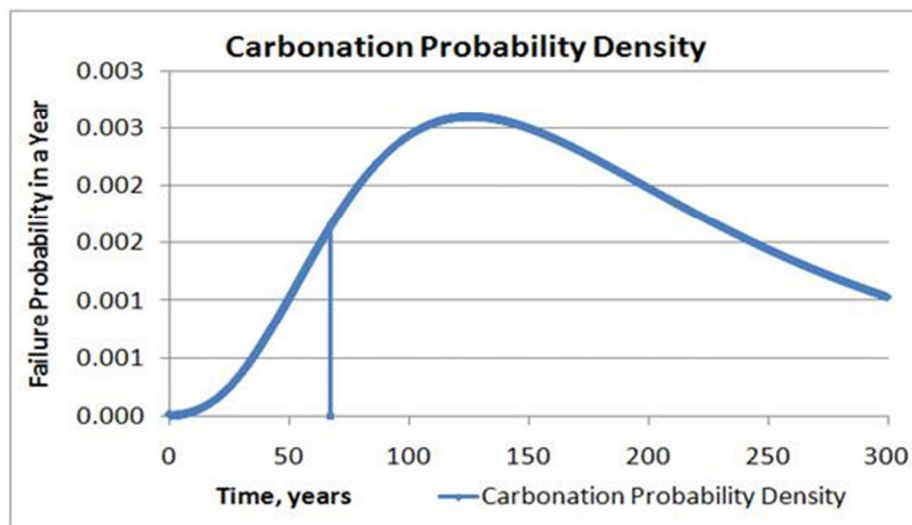
Figure 4.1   Graphical Representation of Probability Density of Carbonation of Imitation Period
Note: Model is based on various input parameters and is only to demonstrate form of the graph

To estimate the propagation time of corrosion on the basis of cracking of the concrete cover the following formula is utilized

$$t_1 = 80 \left(\frac{c}{dr} \right)$$ Equation 4-3

d = diameter of rebar, mm

r = rate of corrosion in rebar, μm/year

c = thickness of concrete cover, mm

The mean rate of corrosion in carbonated concrete can be taken as 5-10 μm/year and 2μm/year at 90-98% and less that 85% relative humidity respectively (Parameswaran, et al. 2008). As depicted in Figure 4.2, it is evident that the initiation time for carbonation to reach the depth of an average concrete cover (50mm) may last longer than the service life of the structure itself.
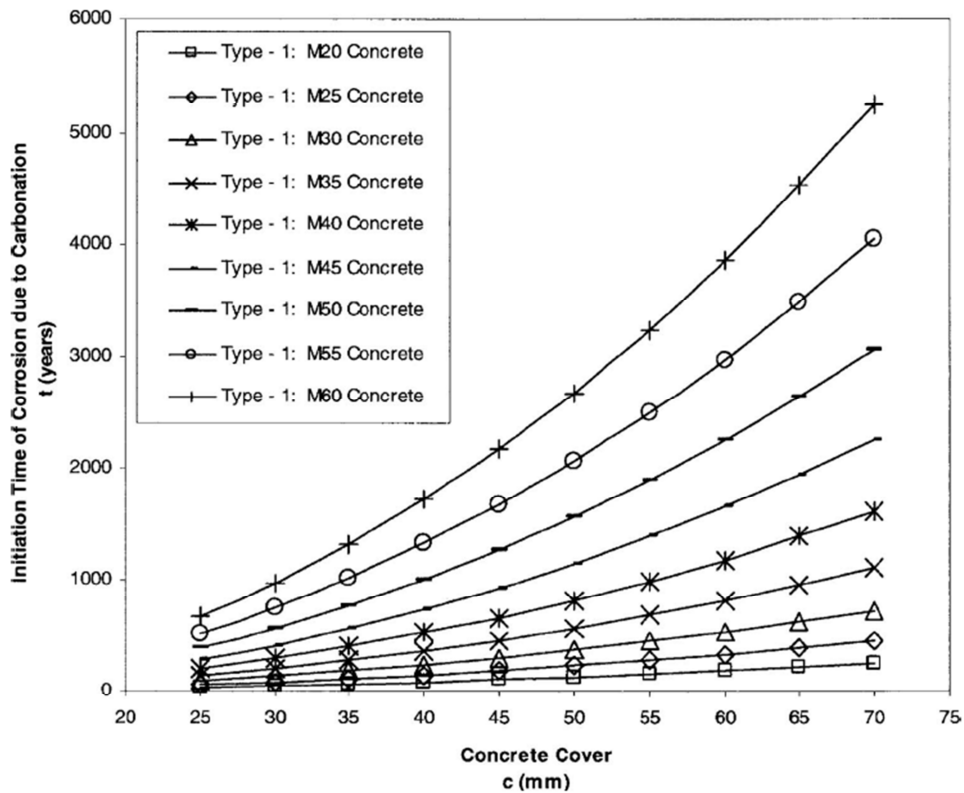
Figure 4.2   Effect of Concrete Cover Depth on Initiation Time of Corrosion for concrete with Type 1 binder (air entrained, not exposed to rain) (Parameswaran, et al. 2008).

5. Chloride Contamination

Chloride contamination in concrete is a frequent cause of corrosion of reinforcing steel. Chloride may be added to the concrete as impurities of the constituent materials. Both free and bound chlorides exist in concrete. However, the chloride-induced corrosion process is related to only the free chlorides since the bounded chloride is immovable and cannot initiation corrosion (Chen and Mahadevan, 2008). In some structures in the past, chloride was added to concrete as an accelerating admixture, such as calcium chloride (Poulsen, 2006). However, this practice is forbidden today and the main source of chloride in concrete penetration comes from external sources: de-icing salts and marine environmental conditions.

While not all de-icing salts contain chloride, sodium chloride (NaCl) is the cheapest and most efficient de-icing salt, and is therefore commonly used. As the salt breaks down the ice, the concrete is exposed to the chloride through the melting water. Bridges are subjected to chlorides after de-icing salts are transferred from the road by travelling vehicles. Seawater and brackish water contain substances which are also aggressive against concrete and steel reinforcement. For marine exposure conditions, chloride can be defined to derive from the following four environmental zones (Poulsen, 2006), which are illustrated in Figure 5.1:

- o **Marine atmosphere Zone (ATM) -**Concrete is positioned above the highest maximum water level, including waves.
- o **Marine Splash Zone (SPL) -**Concrete is spaced between the highest maximum water level including waves, but still above the mean water level height.

- o **Tidal Zone –** The Tidal zone should be considered with data from the Splash zone and the Submerged Zone.
- o **Submerged Zone (SUB) -** Concrete is submerged in seawater, below the lowest water level.
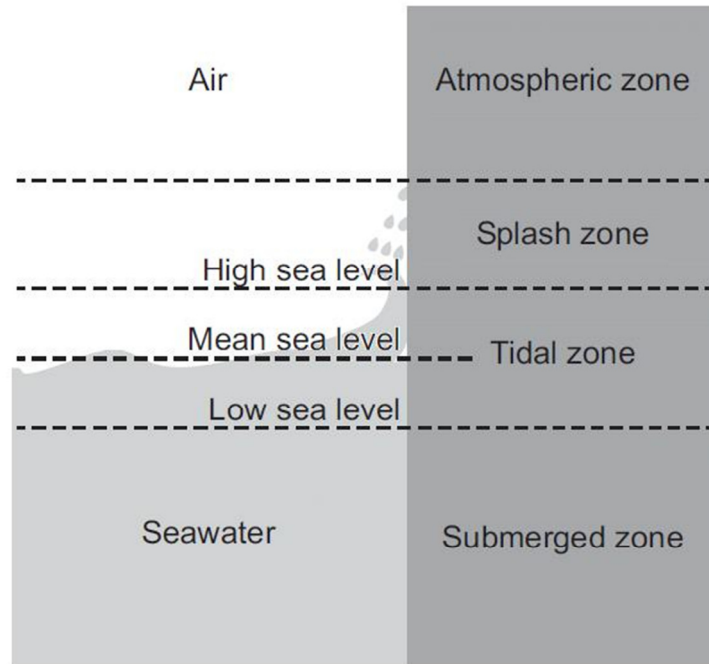
Figure 5.1   Environmental Zones of Marine Exposure (Bertolini et al., 2004)

Chloride penetration from the environment produces a profile in the concrete characterized by high chloride content near the external surface and decreasing contents at greater depths. The chloride profile also acts as the basis in characterizing the chloride diffusivity of concrete. The theoretical profile and one-dimensional chloride ion diffusion process in concrete can be viewed as following Fick's Second Law of Diffusion:

$$\frac{\partial C(x,t)}{\partial t} = D \frac{\partial^2 C(x,t)}{(\partial x)^2} \qquad \text{Equation 5-1}$$

In general, Fick's Second Law predicts how diffusion causes the concentration amounts to change with time. Typical the chloride diffusion coefficient is dependent on the location x, time

t and the chloride concentration. However, it is often acceptable to ignore the dependency of the

location. Therefore, the following conditions can be developed from our knowledge of chloride

diffusion in concrete:

Initial Condition: $C(x > 0, t = 0) = 0$

Boundary Condition: $C(x = 0, t > 0) = C_s$

Closed form solution: $C(x,t) = C_s \left\{ 1 - \text{erf}\left(\frac{x}{2\sqrt{D_c t}} \right) \right\}$ Equation 5-2

C_s -Surface Chloride Content (kg/m^3 or % by wt. of cement) at x = 0
$C(x,t)$ –Concentration of free chlorides (kg/m^3 or % by wt. of cement) at depth x and time t
erf –error function
D_c -diffusion coefficient (m^2/s)
t –time (s)
x –depth (m)

From the rate equation for $C(x,t)$, we can develop a similar graphical relation that expresses the

percent of chloride content vs. the time period of exposure, as seen in Figure 5.2. This

correlation is independent from the cover depth, which represent the different color lines.

From the graph, it is also evident that the longer period of exposure then the higher percent of

chloride content.
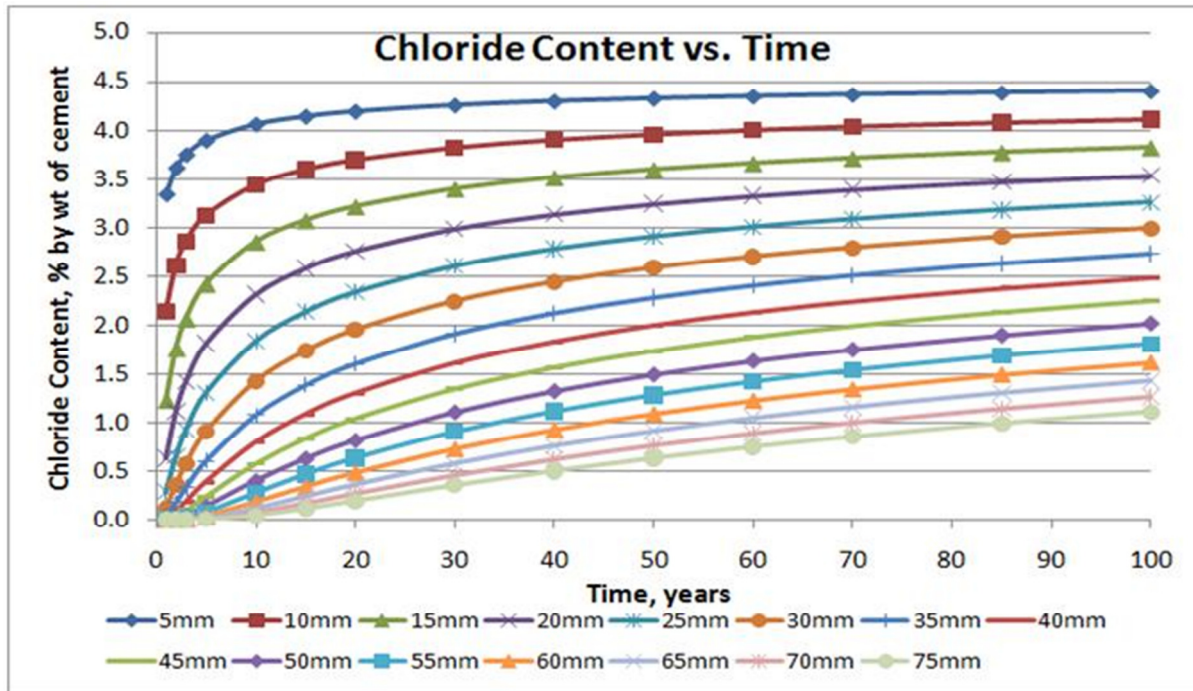
Figure 5.2   Chloride Content vs. Time of Exposure

Note: Model is based on various input parameters and is only to demonstrate form of the graph

Chloride content is typically given in units of % mass of cement. However, sometimes the

chloride content is given in % mass of concrete. The following conversion can be used (CTI

Consultants, 2004):

% chloride by mass/wt. concrete $* \frac{\text{density of concrete}}{\text{density of cement}} = $ % chloride by mass/wt. of cement

<div align="right">Equation 5-3</div>

Where
Density of normal concrete is 150lbs/ft^3 or 2400 kg/m^3
Density cement has a minimum cement content of 350kg/m$^3 \rightarrow$ 400kg/m^3 (including fly ash)

Where the chloride content is only reported as a percentage by weight of concrete sample and the

mix proportions are not reported, a cement content of 350 kg/m^3 and a sample density of 2300

kg/m^3 have been assumed (Glass et al. 1997).

26

5.1   Chloride Threshold Value

Initiation of corrosion takes place when the chloride content at the surface of the reinforcement reaches this *threshold value* (or critical chloride content). A certain time is required from the breakdown of the passive film on the reinforcement and the formation of the first pit within the reinforcement. Pitting of the reinforcement is essentially the start of the corrosion process. Therefore, the chloride threshold value can be briefly summarized as the concentration of chloride required to initiate corrosion of steel reinforcement. While the threshold value depends on several parameters, a major influence is from the amount of oxygen that can reach the reinforcement. Therefore, a structure exposed to the atmosphere is more susceptible to corrosion initiation, opposed to a structure that is immersed in seawater, which would need much higher levels of chloride content.   With the environmental conditions involved, the threshold of chloride in concrete is not a distinct amount. The idea of having a single value determine if corrosion initiates on reinforcement is not rational (Life365 User Manual, 2008). Nevertheless, typical values of chloride that have caused extensive damage in concrete have ranged from .2% to .4% by wt. of cement for severe and moderate conditions, respectively (CTI Consultants, 2004). For normal performance concrete, a value of .4% may usually be considered, but even lower values are possible for certain concretes and exposure conditions (Bertolini, 2004).

As illustrated in Table 5.2, both Bamforth and Life-365 use chloride threshold values of .4% by wt. of cement. However, Lounis and Daigle found that threshold chloride content typically used in North America as 0.6 kg/m^3 to 0.9 kg/m^3 or 0.17% to 0.26% by wt. of cement, assuming the typical cement content of 350 kg/m^3 (Lounis and Daigle, 2008). Stewart and Rosowsky compile statistical parameters and utilize the mean value of .9kg/m^3 (Stewart and Rosowsky, 1998).

Furthermore, Frederiksen et al. (1997) propose that the threshold value depends on the concrete composition, as seen in equation:

$$C_{cr} = k_{cr} \; x \; \exp(-1.5 \; x \; eqv \; \{w/c_{cr}\}) \qquad\qquad \text{Equation 5-4}$$

Where,

$$w/c_{cr} = \frac{W}{PC + f_{fa} xFA + f_{sf} xSF} = \frac{W}{PC} \quad \text{(No FA or SF)} \qquad \text{Equation 5-5}$$

	Efficiency Factors, f	Environmental Factors, k_{cr}
Portland Cement, PC	+1.0	1.25
Silica Fume, SF	-4.7	1.25
Fly ash, FA	-1.4	3.35

Table 5.1   Efficiency Factors and Environmental Factors (Poulsen, 2006)

Table 5.2 illustrates the proposed threshold values from experimental observations and research performed.

	Lounis & Daigle, 2008	Stewart & Rosowsky, 1998	Life-365, 2010	Bamforth, 1998	Frederiksen et al, 1997
Threshold Chloride Content, % by wt of cement	0.2	0.257	0.4	0.4	0.64
Typical Range	.17 → .26	.17 → .34	---	---	---
Threshold Chloride Content, kg/m³	0.7	0.9	1.4	1.4	2.23
Typical Range	.6 → .9	.6 → 1.2	---	---	---

Table 5.2   Typical Threshold Chloride Content Values

The relationship between the chloride threshold value and the amount of chloride at the steel surface can be modeled together if the probability densities are known. On the same plot, the threshold chloride value and chloride content at the steel surface provide the probabilistic area of corrosion initiation. In line with probabilistic modeling, the chloride amount on the steel would act as the "loading" applied to the structure and the threshold value would act as the amount of

resistance the structure can provide.   Thus the probability of failure, or probability of corrosion

initiation, is described as:

$$P_f(t) = P\{R(t) < S(t)\} = P\{C_{th} < C_{st}\} \qquad \text{Equation 5-6}$$

As seen in the illustration of Figure 5.3, if after a certain period of time the mean value of the

chloride concentration at the steel level, C_{st} is found much lower than the threshold value, C_{th},

then the model predicts no corrosion.
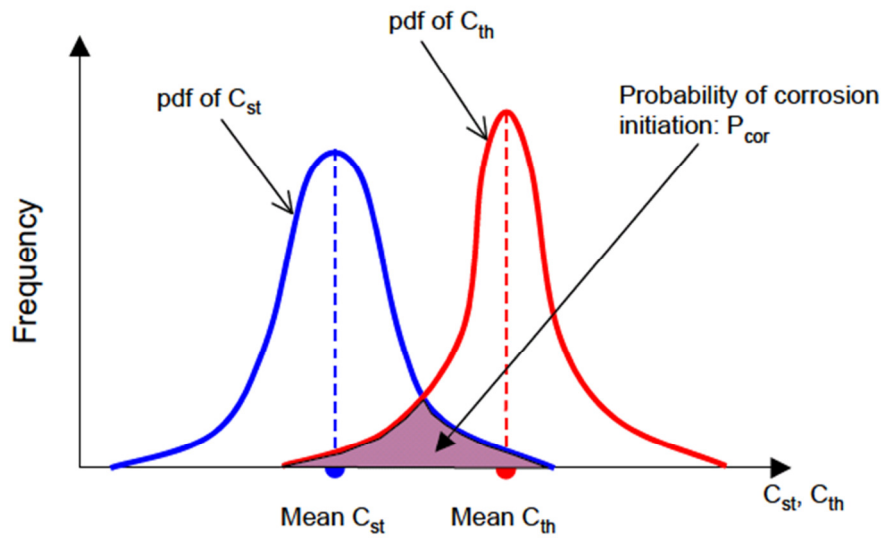
Figure 5.3   Probability of Corrosion before Chlorides Amounts Surpass Threshold

(Lounis and Daigle, 2008)

Using the real-life statistical parameters, shown in Table 5.3 and provided by Lounis and Daigle, the relationship can be further observed, which is illustrated in Figure 5.4.

Parameter	Mean value	COV* (%)
Concrete cover depth (mm)	70	25
Bar spacing (mm)	150	5
Bar diameter (mm)	9.5	-
Surface chloride content (kg/m^3)	6	25
Chloride (apparent) coefficient of diffusion (cm^2/year) - **NPC**	0.40	25
Chloride (apparent) coefficient of diffusion (cm^2/year) – **HPC**	0.20	25
Threshold chloride content (kg/m^3)	0.70	20
Corrosion rate (µA/cm^2)	0.5	20

*COV = coefficient of variation

Table 5.3   Service Life Parameters (Lounis and Daigle, 2008)
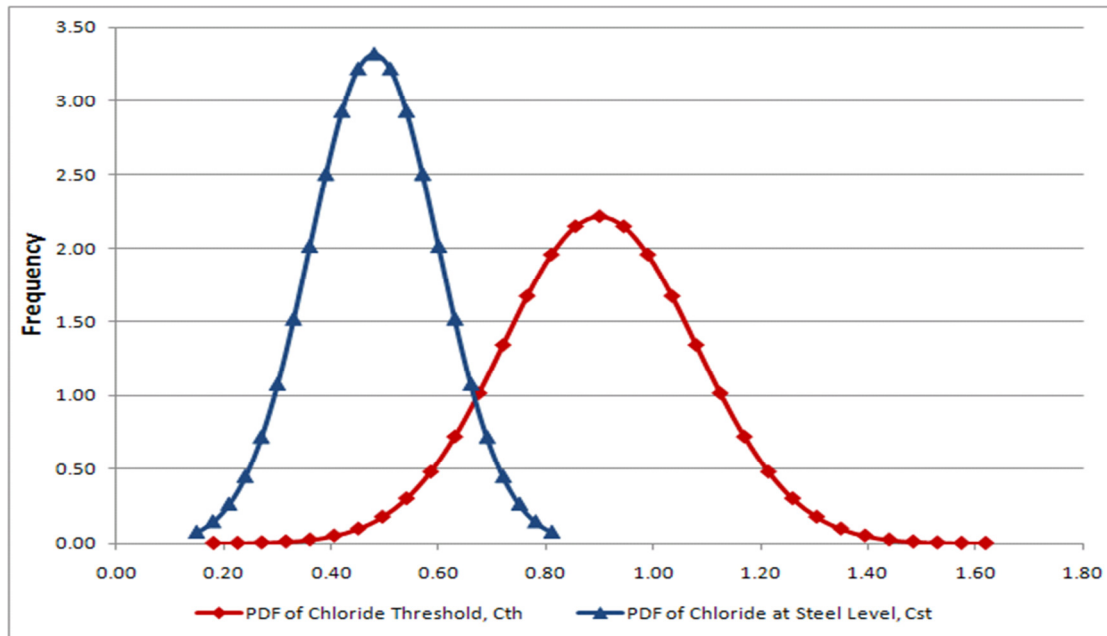
Figure 5.4   Probability of Corrosion with Lounis & Daigle Service Life Parameters for t=20 years

5.2 Chloride Surface Content

The surface chloride, C_s, is a measurement of the amount of chloride on the surface of the concrete structure. The highest values of surface chloride content are found in splash zones where the water evaporation and wet dry cycling causes an accumulation of chloride. At a shallow depth, the chloride concentration reaches a maximum value that can be assumed constant after an initial exposure time. In experimentation and in the field, the surface chloride value is generally obtained from regression analysis of various chloride profiles (Weyers et al. 1994). The amount of surface chlorides will significantly affect the chloride penetration, which is a complex function of position, environment and concrete properties.

It is primarily under diverse environmental conditions that C_s will have different values. Bamforth gathered information on concrete blocks exposed to de-icing salt applications along a motorway in the UK. From gathering this information for nine years, Bamforth determined that C_s increases over several years, with normal values corresponding to 3 to 4% by mass of cement (Bamforth, 1997).

Frederiksen et al. (1997) also studied chloride observations from the Traslovslage Marine Exposure Station, and concluded that the surface chloride content after 1 year of exposure can be expressed by the relation,

$$C_1 = k_b \; x \; eqv \; \{w/c_b\} \qquad \text{Equation 5-7}$$

Where eqv $\{w/c_b\}$ is determined by

$$eqv \; \{w/c_b\} = \frac{W}{PC + 0.75xFA - 1.55xSF} = \frac{W}{PC} \quad \text{(No FA or SF)} \qquad \text{Equation 5-8}$$

And k_b is determined by

Concrete Environment	Factor, k_b
Concrete exposed to marine atmosphere (ATM)	2.20
Concrete exposed to marine splash zone (SPL)	3.67
Concrete submerged in seawater (SUB)	5.13

Table 5.4   Factor k_b (Frederiksen *et al.* (1997))

With the first year surface chloride content known, Frederiksen also proposed a way of

determining the surface content for a specified exposure period. Frederiksen observations found

that the surface chloride content will increase by a factor of 7 after 100 years of exposure. The

following relationship was developed,

$$C_{100} = k_{100} \ x \ C_1$$ Equation 5-9

And k_{100} is determined by

Concrete Environment	Factor, k_{100}
Concrete exposed to marine atmosphere (ATM)	7.00
Concrete exposed to marine splash zone (SPL)	4.50
Concrete submerged in seawater (SUB)	1.50

Table 5.5   Factor for Surface Chloride Content after 100 years of Exposure
(Frederiksen *et al.* (1997))

With the known values for the surface chloride content after 1 year and after 100 years,

Frederiksen established a relationship to find the surface chloride content at any time period,

$$C_{sa} = C_i + \ S_1(t/t_1)^{(1-\alpha)p}$$ Equation 5-10

Where,
t_1 = 1 year
C_i = uniformly distributed chloride content of the concrete, typically assumed = 0
α and *p* are factors that depend on the composition of concrete and environment (shown below)
$S_1 = C_1 - C_i$

$$p = \frac{\log_{10}(C_{100}-C_i)-\log_{10}(C_1-C_i)}{2(1-\alpha)}$$ Equation 5-11

$$\alpha = k_\alpha(1 - 1.5(w/c_D))$$ Equation 5-12

32

Concrete Environment	Factor, k_a
Concrete exposed to marine atmosphere (ATM)	1
Concrete exposed to marine splash zone (SPL)	.1
Concrete submerged in seawater (SUB)	.6

Table 5.6   Factors for Age Parameter (Frederiksen *et al.* (1997))

Life-365 uses a geographic model to determine a maximum surface chloride concentration, C_s, and the time taken to reach that maximum, t_{max}, based on the type of structure and its geographic location. This model, found in Figure 5.5, was created from surveys performed by the Salt Institute between 1960 and 1984, and data related to the chloride build up rate for U.S. highways from Weyers et al. 1993 (Life365 User Manual, 2010).
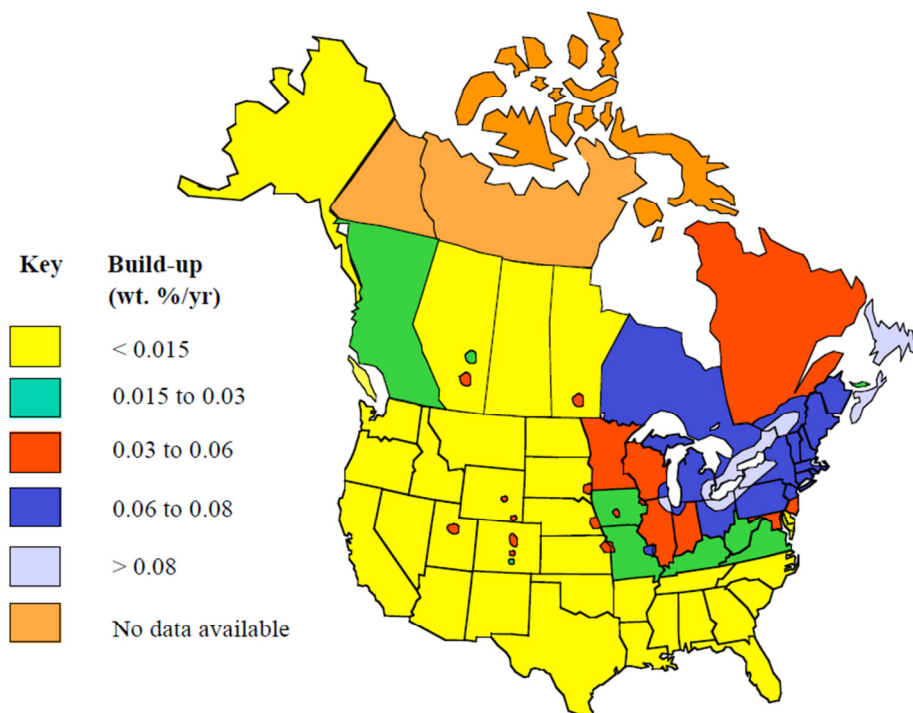
Figure 5.5   Surface Chloride Levels in North America (Life-365 User manual, 2010)

Table 5.7 illustrates the proposed surface chloride values from experimental observations and

research performed.

	Lounis & Daigle, 2008	Stewart & Rosowsky, 1998	Life-365, 2010	Bamforth, 1998	Frederiksen et al. 1997
Surface Chloride Content, % by wt of cement	1.71	1	4.8	4.80	4.70
Surface Chloride Content, kg/m^3	6	3.5	16.8	16.8	16.45

Table 5.7   Typical Threshold Chloride Content Values

5.3　Diffusion

While there are multiple ways for the transport of chloride in concrete, diffusion is the primary transport mechanism and is used for analysis. The diffusion coefficient illustrates the material properties (water-to-cement ratio, temperature, cement type, and age) of concrete and reflects the ability of concrete to resist chloride penetration. Research has indicated that the chloride diffusion coefficient decreases with time due to the increase in maturity of the exposed concrete. An apparent value of the diffusion coefficient can be obtained in the field from cored concrete samples, which would be an accurate representation of the concrete properties (Lounis and Daigle, 2008). The variation of chloride diffusion coefficients found in the literature may be due to the difference in how they were obtained. Chloride diffusion coefficients may be:

- o measured in the laboratory

- o in outdoor testing conditions

- o taken from field measurements

Therefore, diffusion coefficient values can vary by more than one order of magnitude due to the diversity of the mixes tested and difference in ages, curing and testing conditions. In general, many researchers agree upon the following mathematical description of the diffusion coefficient:

$$\mathbf{D(t)} = \mathbf{D_{ref}} \left(\frac{t_{ref}}{t}\right)^{m} = \mathbf{D_{ref}} \left(\frac{t}{t_{ref}}\right)^{-m} \qquad\qquad \text{Equation 5-13}$$

D(t) - effective diffusion coefficient (m^2/s), often written as *D*
D_{ref} - apparent diffusion coefficient (m^2/s)
T_{re} - time at which the apparent diffusion coefficient is found (years)
t - time the structure has been in service (years)
m - age reduction factor

The age factor is dependent on the concrete mixed proportions, such as the additional admixtures of fly ash and slag, and the type of curing applied to the concrete. The following equation is proposed and utilized by Life-365 to modify *m* (after 28 days of exposure) based on the level of fly ash (%FA) or slag (%SG)

$$m = 0.2 + 0.4(\%FA/50 + \%SG/70) \qquad \text{Equation 5-14}$$

This relationship is only valid up to the replacement levels of 50% fly ash or 70% slag and *n* itself cannot exceed .6 (the max value if the fly ash and slag were used at 50% and 70% respectively). Life-365 will not compute the diffusion values for higher levels of the materials (fly ash and slag). Figure 5.6 illustrates the affects of fly ash and slag on the diffusion coefficient. After 25 years, Life-365 holds the value of m at a constant value to show that hydration in the concrete is complete.
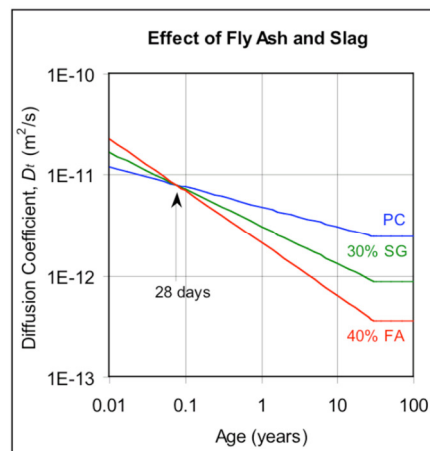
Figure 5.6   Effects of Fly Ash and Slag on the Diffusion Coefficient
(Life365 User Manual, 2010)

Bamforth proposed the age factor design values (in Table 5.8) after analyzing published data from various concrete types. The age factors derived from Bamforth represent values expected after 20 years of exposure (Bamforth, 1998). Bamforth's data was mainly gathered from marine

studies where there is a constant supply of moisture. This age reduction factor was originally

used in the chloride diffusion spreadsheet.

Concrete Mixture	Bamforth's Age Reduction Factor, m	Life-365, m (m <=0.60)
PC Concrete	.264	.20
Fly Ash Concrete	.700	.37
Slag	.6	.5

Table 5.8   Representative Values of the Age Reduction Factor

(Bamforth, 1998) & (Life-365 User Manual, 2010)

Diffusion Coefficient proposed by Life-365 (Life-365 User Manual, 2010)

$$D = D_{28} \left(\frac{t_{ref}}{t} \right)^m$$
Equation 5-15

D_{28} - diffusion coefficient at time t_{28} (= 28 days in Life-365)

$\qquad D_{28} = 10^{-12.06\ +\ 2.40 w/cm}$ (m^2/s)

t - time in service, days

t_{ref} - 28 days

m - diffusion decay index, a constant

The relationship between D_{28} and the water-cementitious materials ratio (*w/cm*) (Figure 5.7) is

based on a large database of bulk diffusion tests adopted from the Norwegian standard method,

where 28 days is the standard laboratory concrete curing time (Life-365 User Manual, 2010).
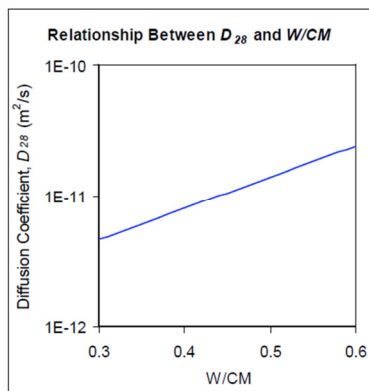
Figure 5.7   Relationship Between D_{28} and w/cm (Life-365 User Manual, 2010)

Diffusion Coefficient proposed by Bamforth (Bamforth, 1998)

In the chloride diffusion spreadsheet, the diffusion coefficient is determined from the equation,

$$D = D_{ca} \left(\frac{t}{t_m}\right)^{-m}$$

D_{ca} - apparent diffusion coefficient (observed from graph)
t_m - 20 years, as the graph is plotted with data of 20 years
t - time in service, years
m - age factor

P.B. Bamforths apparent diffusion coefficient was obtained from the provided log scale graph in Figure 5.8 (Bamforth, 1998). The results in the graph were normalized using an age factor to represent values expected after 20 years of exposure, the time when Bamforth observed some bridges beginning to exhibit problems with rebar corrosion (Bamforth, 1999). From the graph, we find that typical apparent diffusion coefficient values for *w/c* ratios .45 and .5 are approx. 9.4E-13 and 1.25E-12 respectively.
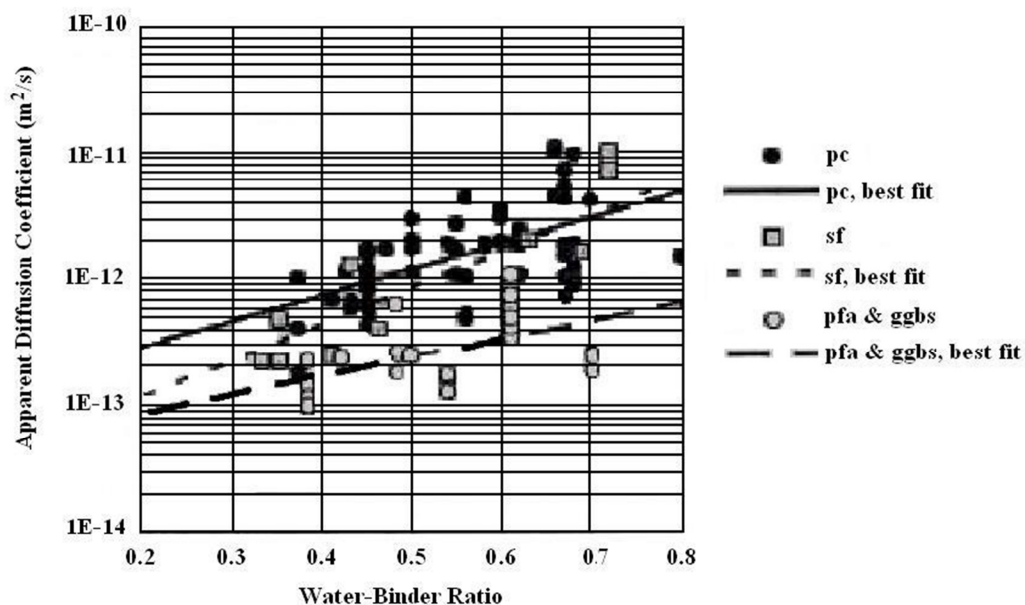
Figure 5.8   Apparent Diffusion Coefficient for Concrete at 20 years of Exposure (Bamforth, 1998).

Diffusion Coefficient proposed by Frederiksen (Frederiksen et al. 1997)

$$D_a(t) = D_1 \left(\frac{t}{t_1}\right)^{-\alpha}$$

D_1 - apparent diffusion coefficient, found 1 year after the first chloride exposure, m^2/s

t_1 - 1 years

t - time in service (time of first chloride exposure of concrete), years

α - age parameter

Age parameter is estimated from equation 5-12 and Table 5.6

The apparent diffusion coefficient after one year exposure was determined from a study of observations from the Traslovslage Marine Exposure Station (Poulsen, 2006). The apparent diffusion coefficient can be solved in the relationship,

$$D_1 = 7.922E^{10} \, k_D e^{-\sqrt{\frac{10}{w/c_D}}} \ m^2/s$$

Concrete Environment	Factor, k_D
Concrete exposed to marine atmosphere (ATM)	.4
Concrete exposed to marine splash zone (SPL)	.6
Concrete submerged in seawater (SUB)	1

Table 5.9   Apparent Diffusion Coefficient Multiplication Factor

Where, eqv {w/c_D} is determined by

$$eqv \, \{w/c_D\} = \frac{W}{PC + FA + 7xSF} = \frac{W}{PC} \quad \text{(No FA or SF)}$$

The effective diffusion coefficient of the four models proposed by Stewart & Rosowsky, Life-365, Frederiksen et al., and Bamforth were graphed in Figure 5.10 where their exponential form could be seen. All models were graphed with a 50 year service life and were converted to the same units of m^2/s. Frederiksen et al., Life-365, and Bamforth's models were created from the proposed equations found in text, and Stewart's model was obtained from computer-integrated

knowledge developed by Bentz et al. 1996. Stewart and Rosowsky analyzed models for the chloride diffusion from 16 separate sources of experimental data and used a least-square fit line to predict the diffusion coefficient, as seen in Figure 5.9 (Stewart and Rosowsky, 1998).
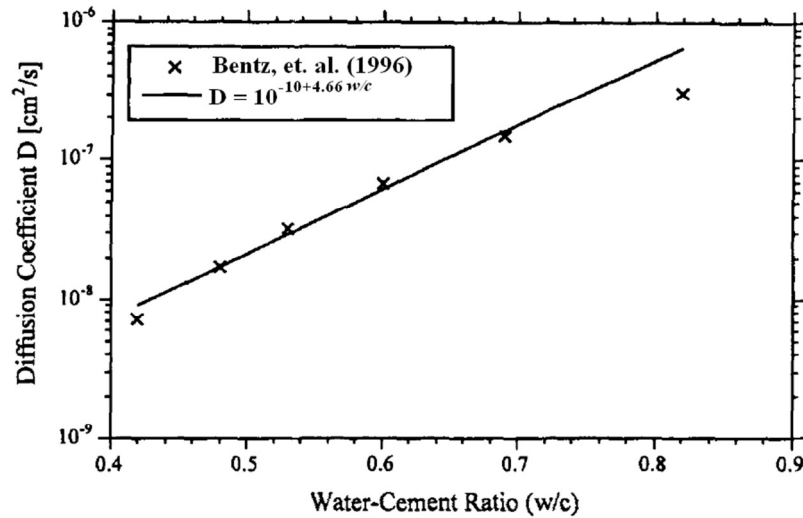
Figure 5.9   Relationship between Water-To-Cement Ratio and Diffusion Coefficient (Stewart and Rosowsky, 1998)

For a given mixed proportion of concrete, the following diffusion coefficient is proposed by Stewart and Rosowsky,

$$D \approx 10^{-10+4.66w/c} \quad cm^2/s \qquad \text{Equation 5-20}$$

Furthermore, when all four exponential models are graphed on a semi-log-normal chart, their linear relationship can also be observed, as illustrated in Figure 5.11. For all four models there is a close relationship between the diffusion coefficient at typical water cement ratios of .45 and .5. Stewart and Rosowsky's curve, which was developed as a mean curve from multiple sets of data, falls in the middle of the other 3 models that are graphed, and continues to be observed as an average for typical water/cement ratios of .45 and .5.   Life-365 gives a higher diffusion coefficient value in an attempt to take a more conservative approach from Bamforth's proposed data. Questioning the validity of its own chosen values, Life-365 encourages users to examine

the influence of *m*: comparing different values in user-defined scenarios (Life365 User Manual,

2010).
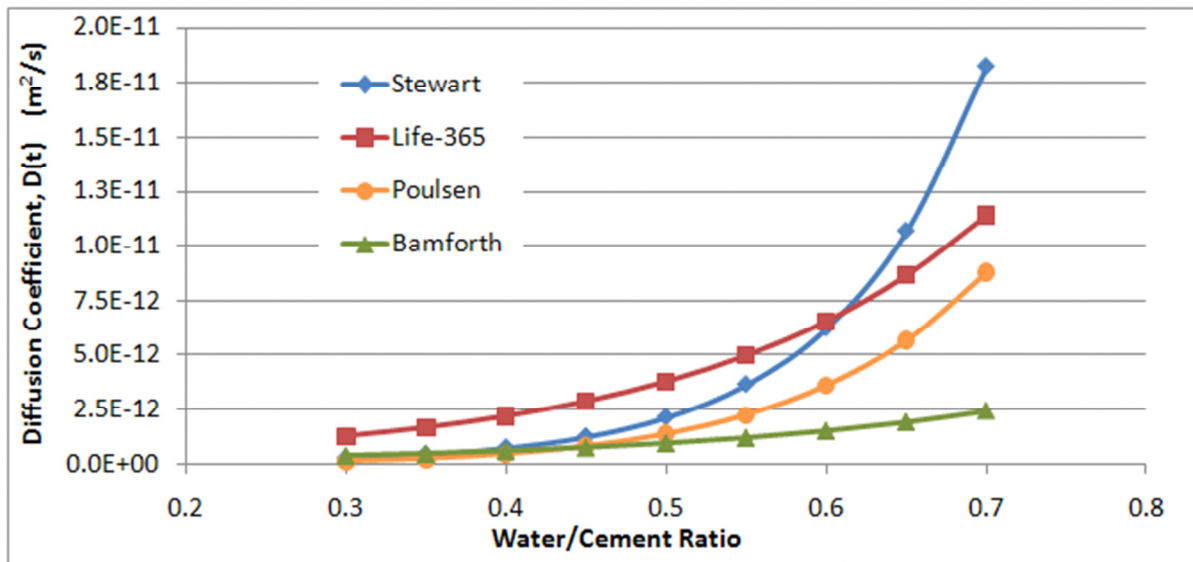
Figure 5.10 Effective Diffusion Coefficients vs. Water/Cement Ratio (t =50 years)
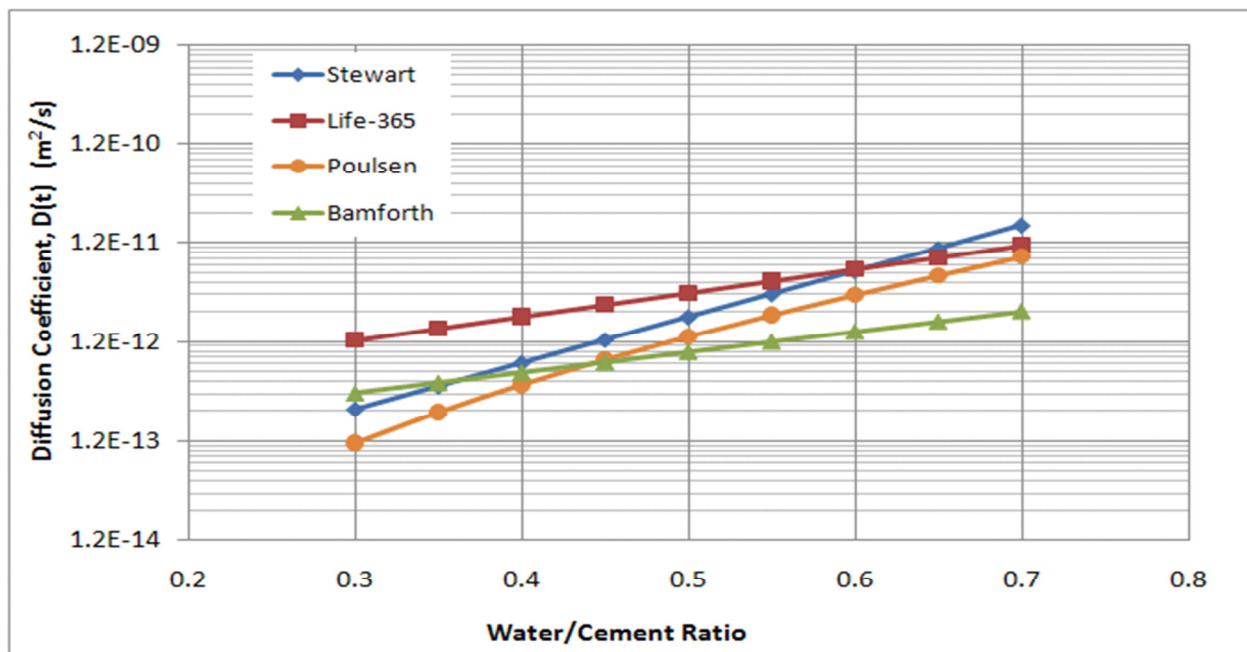
Figure 5.11   Logarithmic Plot of Diffusion Coefficients vs. Water/Cement Ratio (t =50 years)

5.3.1 Differential Equations in Diffusion

Currently, the models for the development of diffusion in concrete are limited to broad specifications or even a one-dimensional diffusion modeling. While one-dimensional diffusion modeling may be sufficient in most cases, other scenarios may call for a more complicated solution when additional conditions are included, such as a time dependent surface chloride ion concentration and diffusion coefficient. The situation of chloride ion diffusion on the corner of a concrete column should also be modeled with two-dimensional modeling to properly account for the amount of chloride ions in concrete.

Therefore, in an attempt to divert from using the closed form solution in equation 5-2, two different solutions to Fick's second law of diffusion have been implemented: the finite difference approximation and the Crank-Nicholson numerical scheme. Rewriting the partial differential equation in terms of finite difference approximations to the derivatives,

Fick's Second Law of Diffusion:
$$\frac{\partial C(x,t)}{\partial t} = D \frac{\partial^2 C(x,t)}{(\partial x)^2}$$
Equation 5-21

$$\frac{\partial C(x,t)}{\partial t} = \frac{C_j^{n+1} - C_j^n}{\Delta t} \qquad D\frac{\partial^2 C(x,t)}{(\partial x)^2} = D\frac{C_{j+1}^n - 2C_j^n + C_{j-1}^n}{\Delta x^2}$$
Equation 5-22

With numerical computation, nonlinear initial chloride ion concentration can be treated in point-wise manner and both the time dependent surface chloride ion concentration and diffusion coefficient can be iteratively updated. Crank-Nicholson numerical scheme: can be used with the finite difference method to illustrate the chloride ion penetration from the outer surface throughout the original concrete.

$$\frac{C_{i,j+1}-C_{i,j}}{\Delta t} = \frac{D}{2}\left[\frac{(C_{i+1,j+1}-2C_{i,j+1}+C_{i-1,j+1})+(C_{i+1,j}-2C_{i,j}+C_{i-1,j})}{(\Delta x)^2}\right]$$
<div align="right">Equation 5-23</div>

Chloride diffusion in the corner of rectangular concrete structures (Figure 5.12) also involves a two-dimensional diffusion process. If it can be assumed that chloride diffusion takes place in parallel planes and that these plans are parallel to the x-y plane, then the following differential equation is utilized:

$$\frac{\partial C(x,t)}{\partial t} = \left(D_x\frac{\partial^2 C(x,t)}{(\partial x)^2} * D_y\frac{\partial^2 C(x,t)}{(\partial y)^2}\right)$$
<div align="right">Equation 5-24</div>
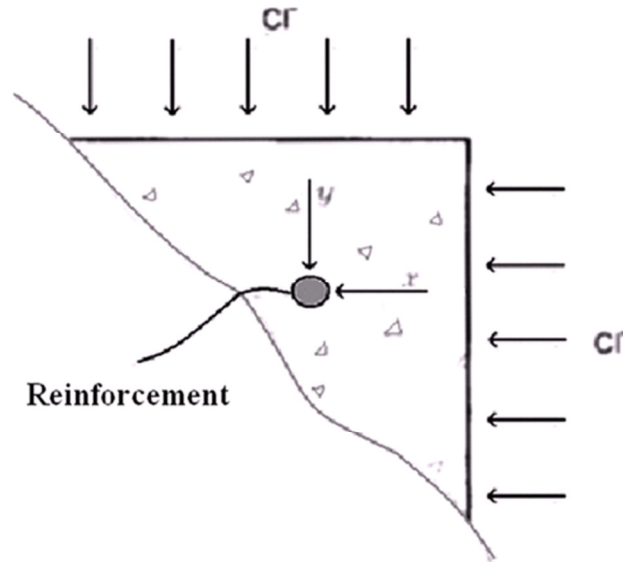
Figure 5.12 Model of 2-D Diffusion Process in Concrete (Shim, 2002)

Life-365 demonstrates another finite difference implementation: the general advection-dispersion equation. Life-365 uses finite differences and the Crank-Nicholson scheme to model both one-dimensional situations (walls and slabs), as well as two-dimensional calculations (square and round columns). Life-365 adopts this approach as a favorable way to predict the future chlorides in concrete as a function of the surface chloride levels.

Therefore, in a one-dimensional scenario the level of chloride at a given slice of the concrete i and next time period $t+1$ is determined by:

$$-ru_{i+1}^{t+1} + (1+2r)u_i^{t+1} - ru_{i-1}^{t+1} = ru_{i+1}^t + (1-2r)ru_i^t + ru_{i-1}^t \qquad \text{Equation 5-25}$$

A two-dimensional scenario determined the initiation period from:

$$(1+2r)u_{i,j}^{t+1} - \frac{r}{2}\left(u_{i-1,j}^{t+1} + u_{i+1,j}^{t+1} + u_{i,j-1}^{t+1} + u_{i,j+1}^{t+1}\right)$$

$$= (1-2r)u_{i,j}^t + \frac{r}{2}\left(u_{i-1,j}^t + u_{i+1,j}^t + u_{i,j-1}^t + u_{i,j+1}^t\right) \qquad \text{Equation 5-26}$$

The one-dimensional calculation by Life-365 has been compared with other calculations and has a strong relationship to them. However, the comparison of initiation period from the two-dimensional calculations has not been validated with accuracy to the other models. The User manual of Life-365 exclaims, "Other sources of validation and further work are necessary to complete the validation of these 1-D and 2-D calculations" (Life-365 User Manual, 2010).

In line with Fick's Second Law of Diffusion, the corrosion initiation time depends on the rate of ingress of chlorides into concrete, surface chloride concentration, depth of concrete cover, and the value of the threshold chloride level. In the case of a chloride attack on a concrete structure, corrosion initiation takes place when a certain critical concentration or threshold value C_{th} is exceeded. However, given that there are some uncertainties in the surface chloride concentration, chloride threshold level and the cover depth, an accurate prediction of the service life or the time to initiation can be difficult to achieve in a deterministic model. Nonetheless, the deterministic model for the time to corrosion can be combined with a probabilistic model to find the characteristic the length of the initiation period.

5.4 Modeling Chloride Initiation Time

The estimation of the initiation period (corrosion-free life) of concrete structures would help bridge engineers with their maintenance plans and allow a means of evaluating the success of various repair alternatives. However, estimating the time to onset of corrosion is not an easy task, but can be estimated through a probability density function. The corrosion initiation time depends on the rate of ingress of chlorides into concrete (diffusion coefficient), the chloride threshold value, the mean surface chloride vales, the depth of the concrete cover.

Rearranging the closed form solution and solving for the time to corrosion:

$$C(x,t)=C_s\left\{1\text{-}erf\left(\frac{x}{2\sqrt{D_ct}}\right)\right\} \quad \rightarrow \quad T_{cr}=\frac{x^2}{4D_T erf^{-1}\left[1\text{-}\frac{C_{th}}{C_s}\right]^2} \qquad \text{Equation 5-27}$$

The initiation period can also be written as,

$$T_{cr}=\frac{x^2}{4D_T erf^{-1}\left[1\text{-}\frac{C_{th}}{C_s}\right]^2} \quad \rightarrow \quad T_{cr}=\left(\frac{c}{k_1}\right)^2 \text{ seconds} \qquad \text{Equation 5-28}$$

Cover depth, c
First year chloride ingress, k_1
Initiation time, t_{cr}
$erf(x)=1\text{-}erfc(x)$
$erf^{-1}(x)=erfc^{-1}(1\text{-}x)$

This equation makes it possible to find the stochastic distribution of initiation time when the concrete cover, c is known and the chloride ingress, k_1 is known.

$$k_1 = 2\sqrt{D_0}\,erfc^{-1}\left(\frac{C_{th}}{C_s}\right) \text{ mm}/\sqrt{\text{year}} \qquad \text{Equation 5-29}$$

From the equations, we can see that there is no assumed correlation between the concrete cover and the first year chloride ingress.

Expectation value of the initiation time of chloride is (Shim, 2002)

$$E[T_{\text{cr}}] = \frac{x^2}{4D_T} \int_{-\infty}^{\infty} \frac{f(C_{th})}{erf^{-1}[1-C_{th}/C_s]^2} dC_{th}$$

The standard deviation of the initiation period of time becomes (Shim, 2002)

$$\sigma_{T_{cr}} = \sqrt{E(T_{cr}^2) - E(T_{cr})^2}$$

Figure 5.13 and Figure 5.14 illustrate the probability density functions from four different sources with water cement ratios =.45 and .5, respectively. The models for Bamforth and Poulsen were derived using their proposed equations and values for normal performance concrete. Lounis and Daigle use mean values from construction specifications and variations estimated from the quality control of workmanship (Lounis and Daigle, 2008). Stewart finds the mean values from various dependable models proposed in the works of other researchers (Stewart and Rosowsky, 1998). From the figures it is evident that there is a strong relationship between models and therefore, the models can provide reliable information on the initiation period.
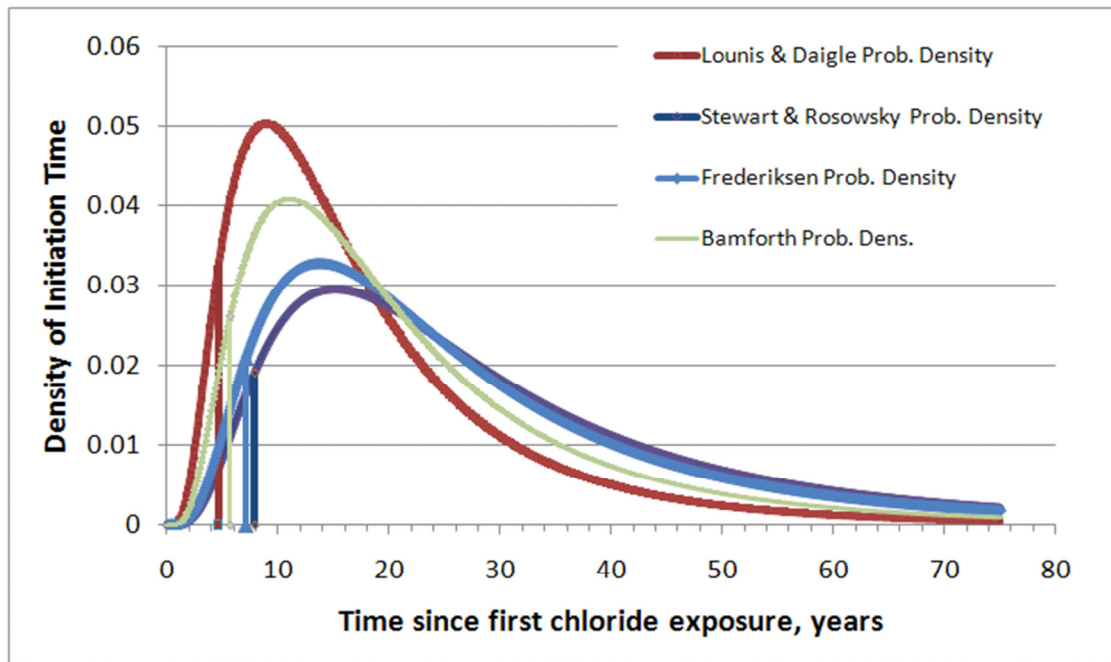
Figure 5.13 Probability Density Function for Initiation Period of Portland Cement with w/c =.45
 Note: Model is based on various input parameters and is only to demonstrate form of the graph
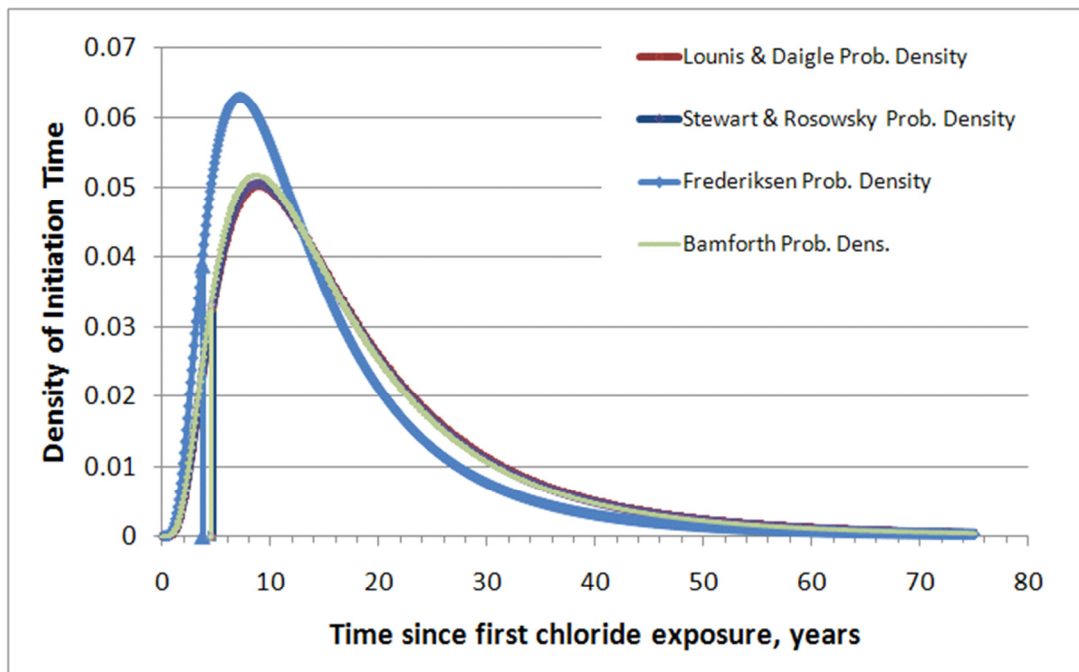
Figure 5.14 Probability Density Function for Initiation Period of Portland Cement with w/c =.5
Note: Model is based on various input parameters and is only to demonstrate form of the graph

6. Chloride Induced Corrosion

Corrosion of steel reinforcement is the most common problem affecting the durability of reinforced concrete structures. Chloride-induced corrosion is one of the main mechanisms of deterioration affecting the service-life and performance of the structure.

Steel reinforcement, embedded in concrete is protected against corrosion by passivation of the steel surface due to the high alkalinity of the concrete. Chloride is a catalyst to corrosion; when a sufficient amount of chlorides reach the reinforcement, the passivation layer is penetrated and the corrosion process will begin. When corrosion takes place, along with the transport of oxygen and water to the steel reinforcement, the steel will oxidize and eventually rust. In other words, the steel dissolves in the pore liquid under the discharge of an electron (Poulsen, 2006). As seen in Figure 6.1, the location of the corrosion is the anode, and in an attempt to stay neutral the reinforcement creates cathodes. The rust products typically have a four to six times the volume of iron, which causes the concrete to expand. Concrete, which is not good in tension, will experience crack growth, delamination, and eventually spalling (Liu and Weyers, 1996).
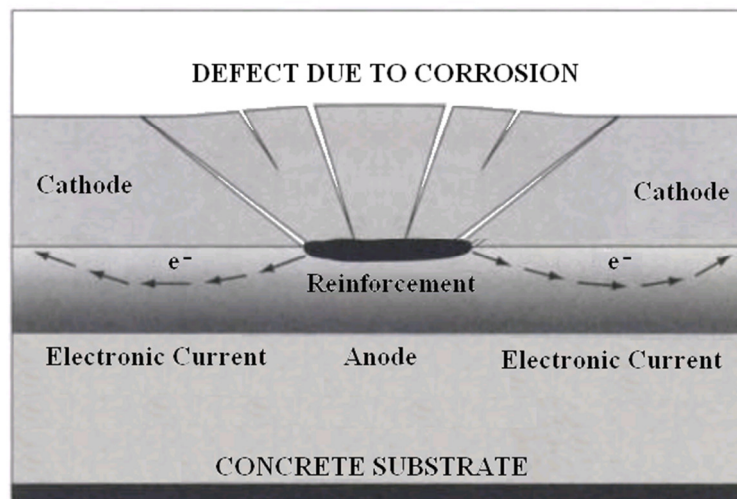
Figure 6.1   Corroded Reinforcement Causes Cracking (Poulsen, 2006)

The extent of corrosion initiation is neither zero nor 100%, as predicted by deterministic models, but is equal to a finite value, which starts at zero at the beginning of the chloride ingress stage and increases with time (Lounis and Daigle, 2008). Therefore, at a given time in the service life, corrosion will be started on a certain amount of the total reinforcing steel while a remaining amount of the reinforcement will be in the passive state. Likewise, for any given period of time, a certain proportion of the structure will experience cracking, delamination or spalling, while the remaining portion of the structure may be damage-free.

6.1 Corrosion Monitoring Techniques

The corrosion of steel embedded in concrete is not visually evident until its effects are seen in the concrete through cracking or spalling. Therefore, nondestructive techniques are developed and used to assess corrosion activity, measure the corrosion rates, and determine the need for repair or rehabilitation.

Along with the half-cell potential, another corrosion detection method is the Linear Polarization Technique. Linear polarization is used to find the corrosion rates of the steel reinforcement. Linear polarization refers to the linear regions of the polarization curve, in which slight changes in current applied to corroding metal in an ionic solution cause corresponding changes in the potential of the metal (Liu, 1996). Therefore, if a large current is required to change the potential to a given amount, the corrosion rate is high; if a small current is required to change the potential the corrosion rate is low. Linear Polarization techniques have been widely used to measure the corrosion current density both in laboratory and in field. Instrument manufacturer's have developed general guidelines for interpreting the results of polarization resistance and corrosion rates, summarized in Table 6.1.

i_{corr} (mA/ft^2)	Corrosion Damage
< 0.2	No damage expected
0.2-1.0	Damage possible 10-15 years
1.0-10.0	Damage possible 2-10 years
> 10.0	Damage possible < 2 years

(Multiply corrosion rate i_{corr} in mA/ft^2 by 1.08 to covert to μA/cm^2)

Table 6.1   Guidelines for Data Interpretation from the Linear Polarization Resistance Technique (Liu, 1996)

6.2 Corrosion Rates

Bamforth originally derived a relationship between the corrosion rate and the chloride content based on experiments with six years of exposure. Bamforth's results concluded that the relationship between the chloride content C_x, and the corrosion rate CR, is an exponential function, which is illustrated in Figure 6.2. In accordance with Bamforth's proposed equations, an exponential function is likely because it is evident that as chloride content accumulates, the corrosion rate would also increase. Bamforth concluded the following relationships were acceptable for their corresponding exposure conditions.

$CR = 0.84e^{0.64C_x}$ - for moderate conditions (wet/rarely dry conditions)

$CR = 0.54e^{1.56C_x}$ - for severe exposure conditions (splash; cyclic wet/dry or airborne seawater)

$CR = 0.46e^{1.84C_x}$ - for very severe exposure conditions (tidal zone conditions)
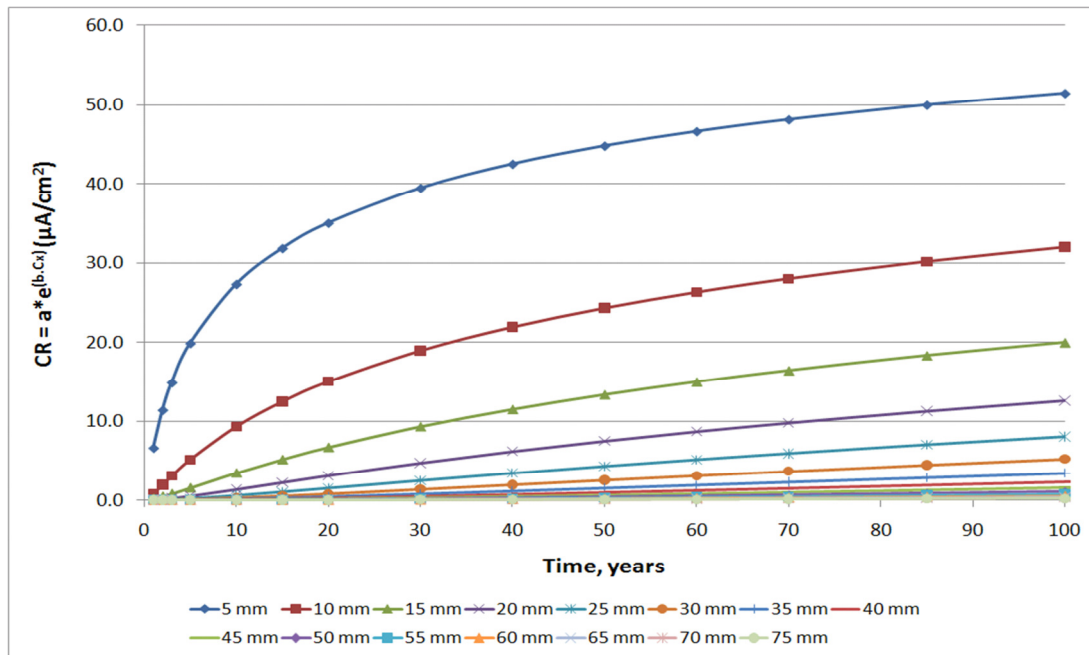
Figure 6.2   Corrosion Rates at Various Depths of Concrete (Bamforth)

Note: Model is based on various input parameters and is only to demonstrate form of the graph

Another empirical approach to the corrosion rate equation was developed by Liu and Weyers, (1998). They examined several factors that affect the corrosion process and used these factors to characterize the corrosion rate. Liu and Weyers model was based on approximately 3000 measurements from 7 series of mixed-in chloride contaminated specimens and up to 5 years of outdoor exposure.   This 5-year corrosion study was obtained from a partial factorial experimental design that simulates reinforced concrete bridges (Markeset, 2008). Liu and Weyers also compared two commercial devices (3LP and Gecor) to measure the corrosion current densities. The values from these devices were compared with corrosion rates from experimental weight loss measurements. Conclusively, Lui developed two non-linear regression models (equations 6-1 and 6-2), which determine corrosion rate from the chloride content, temperature, ohmic resistance, and active corrosion time. Figure 6.3 also illustrates a graphical representation of Liu and Weyers model. From the model we can see that the corrosion rate is going to diverge toward some constant. Stewart proposes that the mean value for the corrosion

rates is 1-2 $\mu A/cm^2$ (Stewart, 1998). As Figure 6.3 illustrates, this is a conceivable value if the unlikely cover depths of 5→30mm were excluded from analysis.

For Acid Soluble Chlorides: (obtained from acid soluble test method (ASTM C1152)

$$\ln 1.08\, i_{corr} = 7.98 + 0.7711 \ln 1.69\, Cl - \frac{3006}{T} - 0.000116 R_c + 2.24 t^{-0.215} \qquad \text{Equation 6-1}$$

For Water Soluble Chlorides:

$$\ln 1.08\, i_{corr} = 8.37 + 0.6180 \ln 1.69\, Cl - \frac{3034}{T} - 0.000105 R_c + 2.32 t^{-0.215} \qquad \text{Equation 6-2}$$

i_{corr} is the corrosion rate, $\mu A/cm^2$
Cl is chloride content, kg/m^3
T is temperature at the depth of steel surface, Kelvin
R_c is ohmic resistance of concrete, Ohms
t is corrosion time, year
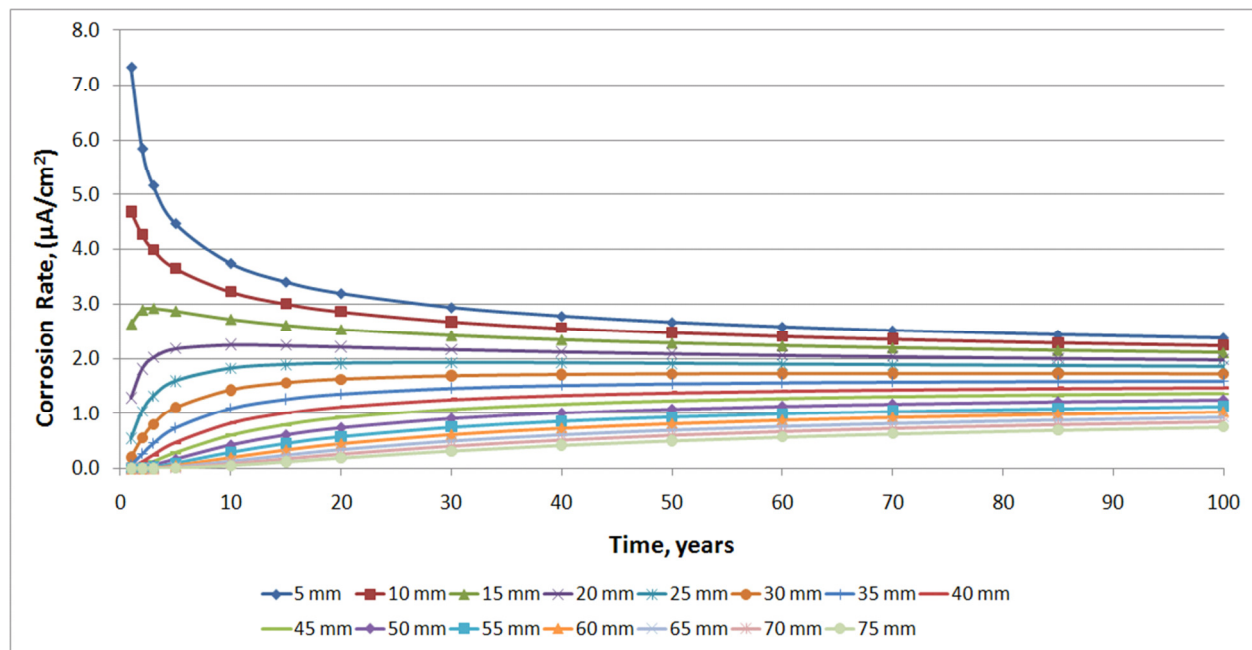
Figure 6.3   Acid Soluble Corrosion Rate at Various Depths of Concrete

Note: Model is based on various input parameters and is only to demonstrate form of the graph

Fick's law demonstrates that chloride concentrations should be given in terms of water-soluble chlorides since it is accepted that the corrosion is primarily influenced by free chlorides and not

binding chlorides. However, as Stewart states, nearly all chloride concentration data in literature refers to acid-soluble chloride concentrations, and therefore the acid-soluble equation is the best used equation. If necessary the relationship between water-soluble chlorides and acid-soluble chlorides was demonstrated by Liu, and can be seen below.

$$C_{water} = aC_{acid} - b$$

where *a* and *b* are coefficients, which mainly depend on amount of cement, type of cement and aggregate used in concrete. For the concrete mix used in Liu's analysis, he found that the values of *a* and *b* equal 0.932 and 0.459, respectively. The relationship between the acid-soluble chlorides and water-soluble chlorides is illustrated in Figure 6.4.
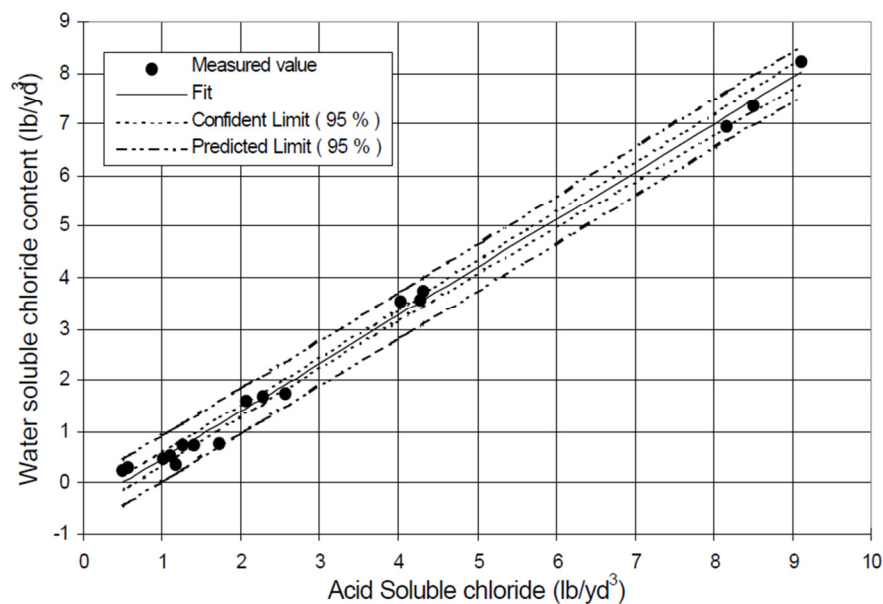
Figure 6.4   Relationships between acid soluble & water soluble chloride content analysis (Liu, 1996)

The corrosion rate of concrete is also affected by electrical resistivity of the concrete, where low resistivity favors the migration of chloride ions and the development of corrosion pits, which are the start to the corrosion process (Arup, 1983). Lui also established a regression relationship between the resistance of concrete and total chloride content for outdoor specimens (Lui, 1996).

This graphical relationship is represented in Figure 6.5, which also illustrates the regression equation between resistivity and chloride content.
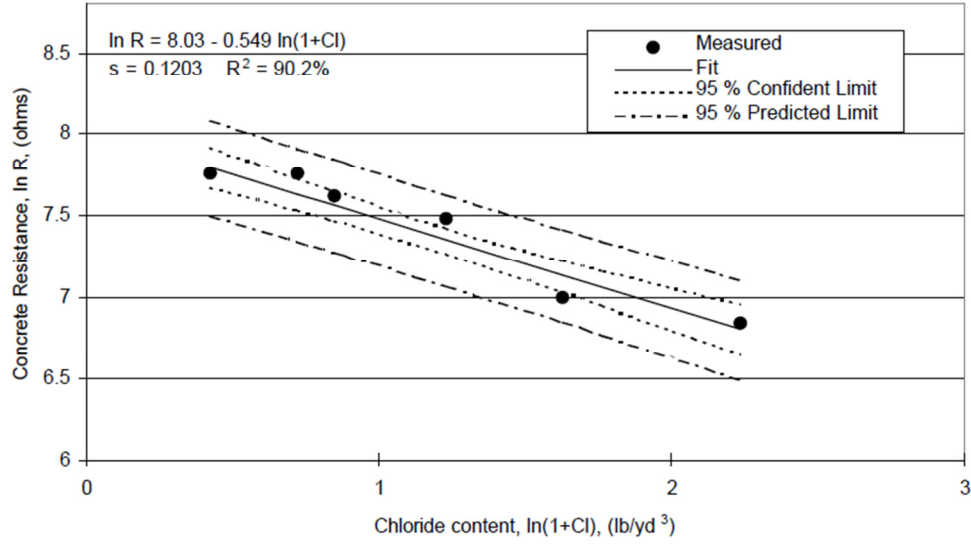
Figure 6.5   Relationship between the Concrete Resistance and Chloride Content (Liu, 1996)

$$\ln R_c = 8.03 - 0.549 \ln(1 + 1.69Cl) \qquad \text{Equation 6-4}$$

$$R_c = e^{(8.03 - 0.549 \ln(1+1.69Cl))} \qquad \text{Equation 6-5}$$

$$R_c = \frac{e^{(8.03)}}{e^{0.549 \ln(1+1.69Cl)}} = \frac{e^{(8.03)}}{(1+1.69Cl)^{0.549}} \qquad \text{Equation 6-6}$$

(Multiply chloride factors in kg/m^3 by 1.69 to convert to lb/yd^3)

Finalized Corrosion Equation for Acid-Soluble Chlorides:

$$\ln 1.08\, i_{corr} = 7.98 + 0.7711 \ln 1.69\, Cl - \frac{3006}{T} - \frac{e^{(8.03)}}{(1+1.69Cl)^{0.549}} + 2.24t^{-0.215} \qquad \text{Equation 6-7}$$

The corrosion rate (i_{corr}) is represented as a current density in µA/cm^2. This can be converted to mm/year: $\lambda \approx 0.0116\, i_{corr}\ (mm/year)$

54

6.3 Calculating Amount of Corrosion

A reinforced concrete substructure is subjected to high compressive strengths, which works as a system between the reinforcing steel and the concrete materials. When the reinforcing steel is subjected to corrosion and/or begins to rust, there is a loss of cross sectional area in the steel reinforcement, thus reducing the capacity of the structure. Therefore, it is important to monitor the amount of corrosion of the steel reinforcement, whether we are monitoring the area of the reinforcement or its yield strength.

In order to assess the reduction in strength of reinforcement, the amount of corrosion must be measured or estimated. The following equation, developed by Du et al. (2005b), is used to make the estimation of the amount of corrosion of reinforcement:

$$Q_{corr} = 0.047 \frac{i_{corr}}{D_b} t \qquad \text{Equation 6-8}$$

i_{corr} = corrosion rate of reinforcement in real structure ($\mu A/cm^2$)
D_b = diameter of no corroded reinforcement, mm
t = time elapsed since the initiation of corrosion, years
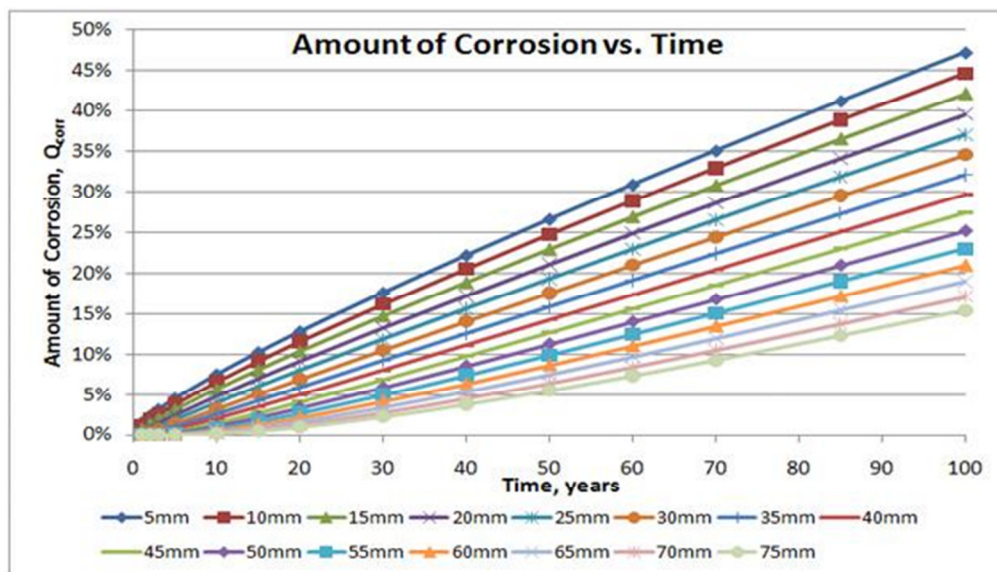
Figure 6.6   Amount Corrosion (%) at Various Cover Depths for the Various Corrosion Rates
Note: Model is based on various input parameters and is only to demonstrate form of the graph

7. Concrete Cracking

Cracking in concrete could develop from stress within the structure or be a product of environmental conditions such as ground movement. If a crack did not appear before corrosion, then cracks will often occur after corrosion initiation. Once rust products from the reinforcement fill the porous zone it results in an expansion of the concrete. As concrete expands, tensile stresses develop in the concrete and with increasing corrosion the cracks will develop.

If we recall the service life model in Figure 7.1, the propagation period is mostly related to the concrete cracking and is dominated by the reinforcement rust expansion during which the rust accumulates on the concrete steel (Chen and Mahadevan, 2007).
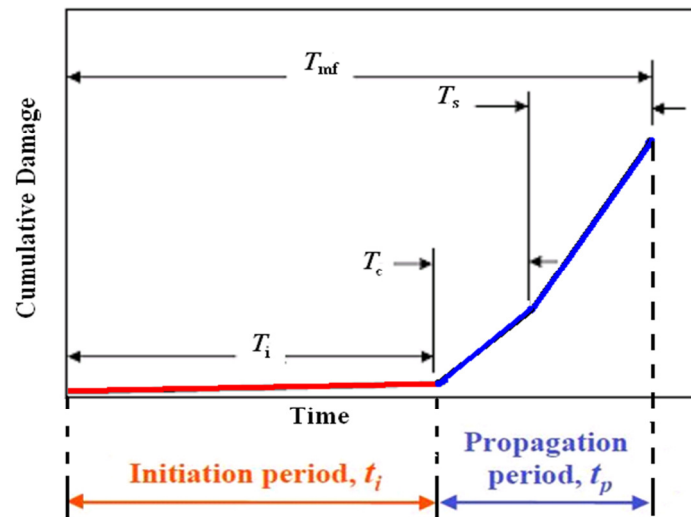
Figure 7.1   Steps of Reinforced Concrete Deterioration due to Chloride-Induced Corrosion (Federal Highway Administration)

Figure 7.2 demonstrates the corrosion process and cracking patterns corresponding to the

following phases:

Phase a: Chloride-penetration and corrosion initiation

Phase b: The corroding steel pits are completely occupied with rust,

Phase c: Further rust products accumulation will trigger expansive stress

Phase d: Surrounding concrete begins to crack until some failure critical mode, such as

spalling or delamination of concrete cover.
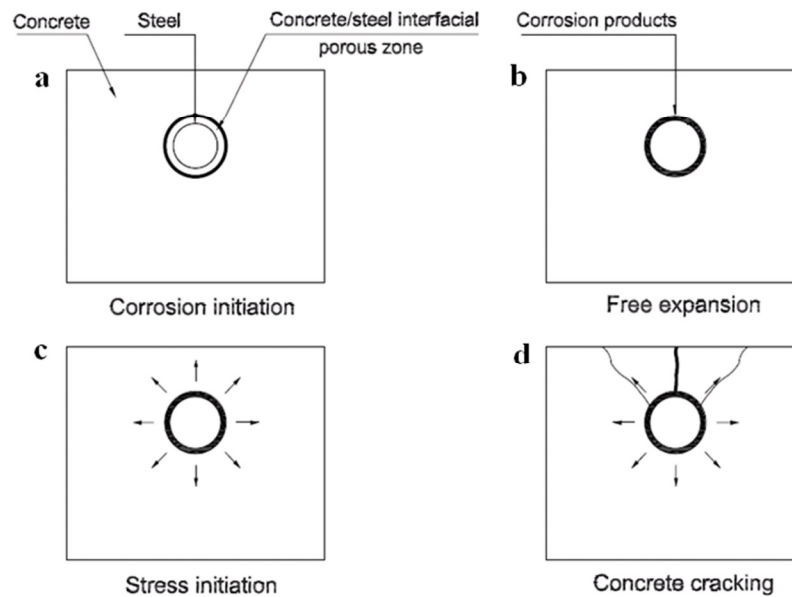
Figure 7.2   Chloride-induced reinforcement corrosion and cracking patterns (Maaddawy and Soudki, 2006).

Regardless if the cracking is due to chloride or other environmental conditions, the crack's width

is important for the assessment of the substructure strength. Depending on the size of the crack

width, the reinforcement can experience small or large changes in its diameter, thus reducing the

strength and capacity of the concrete. The equation, developed by Thoft-Christensen (2004),

relates the reduction in the diameter ΔD to the crack widths Δw, as seen in the equation 7-1,

$$\Delta w = \Delta D \frac{(\alpha-1)\pi D}{\left(\frac{D/2}{D/2+c}+1\right)c}$$

D = original diameter of the steel reinforcement, *mm*

ΔD = change in diameter of steel reinforcement, *mm*

Δw = crack width, *mm*

c = cover depth, *mm*

$\alpha = \rho_{rust}/\rho_{steel}$ ($\rho_r = 0.5\rho_s$) (Maaddawy and Soudki, 2007).

The relationship between the reduction in diameter and the crack with is illustrated in Figure 7.3.

The graphical representation increases linearly to demonstrate an increase in crack width when

the production of corrosion products has increased. This is currently an estimated model, as it

has not been possible on real structures to correlate how the corrosion crack width increases with

time (Thoft-Christensen, 2004).
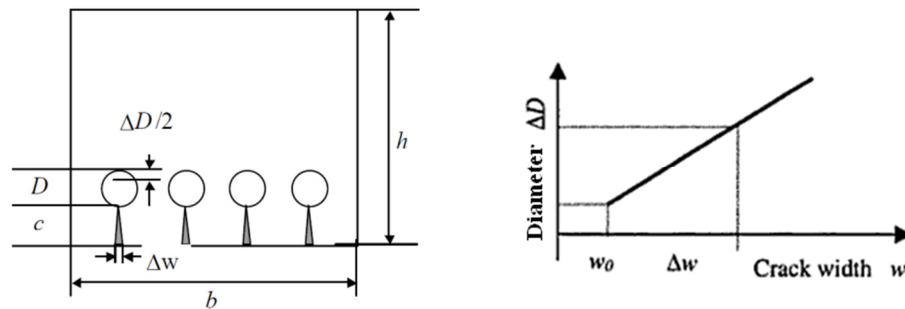
Figure 7.3 Relationship Between the Reduction in Diameter and the Crack Width
(Al-Wazeer, Adel, 2007 and Thoft-Christensen, 2004)

Concrete Crack	1	Crack width $w \leq$ (.004 inch or .1 mm)
	2	Crack width (.004 inch or .1 mm) $< w \leq$ (.012 inch or .3 mm)
	3	Crack width (.012 inch or .3 mm) $< w \leq$ (.024 inch or .6 mm)
	4	Crack width (.024 inch or .6 mm) $< w \leq$ (.04 inch or 1 mm)
	5	Crack width (.04 inch or 1 mm) $< w$

Table 7.1   Classes of Crack Widths

8. Interaction Diagram for Deteriorated RC Pier Columns

Interaction diagrams for columns are generally computed by assuming a series of strain distributions, each corresponding to a particular point on the interaction diagram, and then computing the corresponding values for the load (P) and Moment (M). Once some significant points are computed, the results are summarized in an interaction diagram. The seven points of interest for the interaction diagram are:

- o **Point 1: Zero Moment**
- o **Point 2: Balance Point**
- o **Point 3: Zero Axial Load, Infinite Eccentricity**
- o **Point 4: ε_c = .003 in/in and ε_s = .0030 in/in**   (Equal strain in concrete and steel)
- o **Point 5: ε_c = .003 in/in and ε_s = .0060 in/in**   (Strain in steel 2x strain in concrete)
- o **Point 6: ε_c = .003 in/in and ε_s = .0000 in/in**   (Tension steel has no strain)
- o **Point 7: ε_c = .003 in/in and ε_s = .0005 in/in**   (Very small strain in steel)

As the reinforcement corrosion along the height and cross section of the member leads to a loss of cross section in the reinforcement, the original area and yield strength of the reinforcement no longer applies.
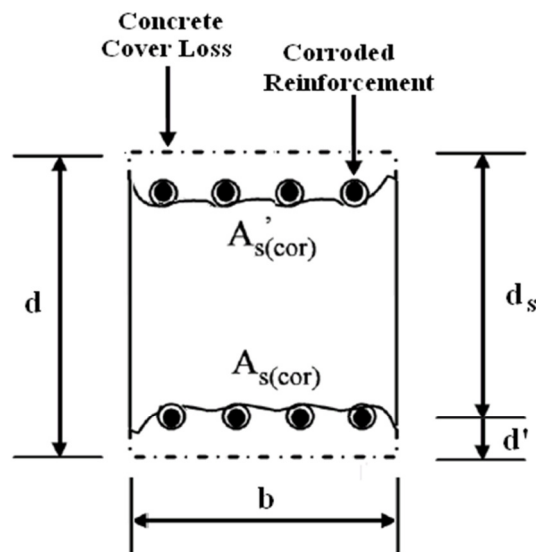
Figure 8.1   Deteriorated Cross Section with reductions in steel and concrete
(Tapan and Aboutaha, 2008)

The area of steel in the interaction diagrams considers both the steel in compression and the steel in tension.

$$A_s = A'_{s(cor)} + A_{s(cor)}$$

The residual capacity of corroded reinforcing bars was investigated by Du et al. (2005a, b). According to Tapan et al. (2008), Du's results agreed reasonably well with corrosion scenarios under natural corrosion conditions. From the distribution of data points in Du's experiments (Figure 8.2 and Figure 8.3), Du proposed the following empirical equations to calculate the residual strengths of the corroded reinforcement,

$$f = (1 - 0.005Q_{corr})f_y$$

$$A_s = (1 - 0.01Q_{corr})A_{s0}$$

f = yield strength of corroded reinforcement ($f_{s(cor)}$)
f_y = yield strength of noncorroded reinforcement
Q_{corr} = amount of corrosion of reinforcement (%)
A_s = average cross-sectional area of corroded reinforcement ($A_{s(cor)}$)
A_{s0} = initial cross-sectional area of noncorroded reinforcement
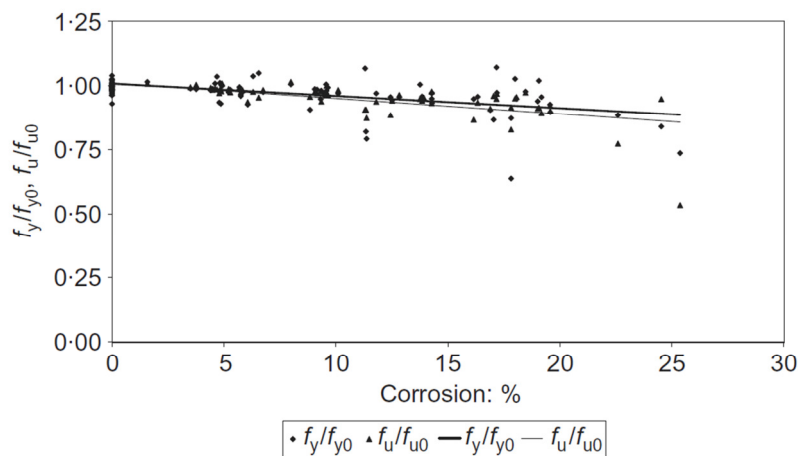
Figure 8.2   Residual forces of corroded bars, used to find equation 8-2 (Du et al. 2005a)
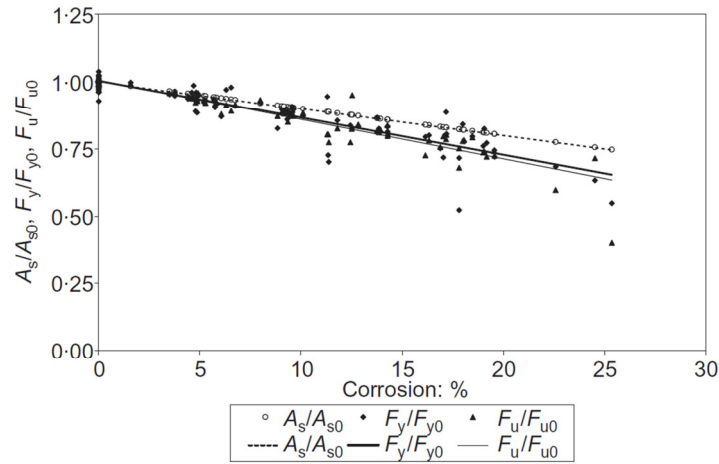
Figure 8.3 Residual forces of corroded bars, used to find equation 8-3 (Du et al. 2005a)

8.1 Proposed Strength Evaluation Model for Deteriorated RC Columns

The proposed structural evaluation procedure for reinforced concrete substructures is based on the development of interaction diagrams using material properties with the reductions from deteriorated reinforcement. In the interaction diagrams, it is assumed that the corrosion of reinforcement does not affect the strength ratio, hardening strain, and elastic modulus of the corroded reinforcement. Therefore, the reinforcement has a stress-strain curve similar to that of non-corroded reinforcement and has a definite yield plateau (Tapan and Aboutaha, 2008). The biggest assumption made is that the corrosion is uniform along the height of the corroded reinforcement. The following calculations demonstrate example points for the interaction diagram.

Interaction Diagram Calculations				
Point 1: Zero Moment			**Capacity Reductions**	
Strain of concrete, ε_c	0.003	in/in	0.003	in/in
Strain of steel, $\varepsilon_s = f_y/E_s$	0.001724	in/in	0.001644	in/in
ACI 10.3.6.1 $P_u = .85 f_c' A_c + A_s f_y$	1328.605	kips	1285.774623	kips
$M_u = \phi A_s f_y (d - a/2)$	0	kip-in	0	kip-in
Point 2: Balance Point				
$\varepsilon'_s = \varepsilon_c (c - d')/c$	0.00224	in/in	0.00225	in/in
$c = d_s (\varepsilon_c/\varepsilon_c + \varepsilon_s)$	9.84	in	10.01	in
$a = .85c$	8.37	in	8.51	in
Compressive steel stress, $f_s' = E_s\varepsilon_s'$	64,903	psi	65,279	psi
Therefore,	Compressive Steel has Yielded		Compressive Steel has Yielded	
$T = A_s f_y$	158	kips	136.6	kips
$C_c = .85f_c' a b_w$	480	kips	488.3	kips
$C_s = A_s' f_y$	158	kips	136.6	kips
$P = C_s + C_c - T$	480	kips	488	kips
Σ Moments @ Plastic Centroid				
$M = C_c(d/2-a/2) + C_s(d/2 - d') + T(d/2 - d')$	377.01	kip-ft	352.42	kip-ft
$e'_{bal} = M/P$	0.785391993		0.721660381	
Point 3: Zero Axial Load, Infinite Eccentricity				
$\rho = \rho' = A_s/b_w d_s$	0.011326165		0.010269904	
$C_c + C_s = T$				
$\{.85 f_c' b_w .85c\} + A_s'[f_s' - .85f_c'] = \{f_y A_s\}$				
$\{.85 f_c' b_w .85c\} + A_s'[E_s \varepsilon_s' - .85f_c'] = \{f_y A_s\}$				
$\{.85 f_c' b_w .85c\} + A_s'[E_s (\varepsilon_c (c - d')/c) - .85f_c'] = \{f_y A_s\}$				
	0	=0	0	=0
c = Using quadratic equation ->	2.81518284	in	2.667311013	in
$a = .85c$	2.392905414	in	2.267214361	in
$\varepsilon'_s = \varepsilon_c (c - d')/c$	0.00087	in/in	0.00075	in/in
Compressive steel stress, $f_s' = E_s\varepsilon_s'$	25,192	psi	21,766	psi
$T = A_s f_y$	158	kips	136.6	kips
$C_c = .85f_c' a b_w$	137	kips	130.1	kips
$C_s = A_s'(f_s' - 0.85f_c')$	69.54	kips	53.2	kips
$P = C_s + C_c - T$	49	kips	47	kips
Σ Moments @ Plastic Centroid				
$M = C_c(d/2-a/2) + C_s(d/2 - d') + T(d/2 - d')$	212.53	kip-ft	188.09	kip-ft

Point 4: $\varepsilon_c = .003$ in/in and $\varepsilon_s = .003$ in/in

Strain of concrete, ε_c	0.003	in/in	0.003	in/in
Strain of steel, ε_s	0.003	in/in	0.003	in/in
$\varepsilon'_s = \varepsilon_c (c - d')/c$	0.00203	in/in	0.00203	in/in
$c = d_s (\varepsilon_c/\varepsilon_c + \varepsilon_s)$	7.75	in	7.75	in
$a = .85c$	6.59	in	6.59	in
Compressive steel stress, $f_s' = E_s\varepsilon_s'$	58,935	psi	58,935	psi
Therefore,	Compressive Steel has Yielded		Compressive Steel has Yielded	
$T = A_s f_y$	158	kips	136.6	kips
$C_c = .85f_c' \, a \, b_w$	378	kips	378.0	kips
$C_s = A_s' f_y$	158	kips	136.6	kips
$P = C_s + C_c - T$	378	kips	378	kips
Σ Moments @ Plastic Centroid				
$M = C_c(d/2-a/2) + C_s(d/2 - d') + T(d/2 - d')$	350.89	kip-ft	327.69	kip-ft

Point 5: $\varepsilon_c = .003$ in/in and $\varepsilon_s = .006$ in/in

Strain of concrete, ε_c	0.003	in/in	0.003	in/in
Strain of steel, ε_s	0.006	in/in	0.006	in/in
$\varepsilon'_s = \varepsilon_c (c - d')/c$	0.00155	in/in	0.00155	in/in
$c = d_s (\varepsilon_c/\varepsilon_c + \varepsilon_s)$	5.17	in	5.17	in
$a = .85c$	4.39	in	4.39	in
Compressive steel stress, $f_s' = E_s\varepsilon_s'$	44,903	psi	44,903	psi
Therefore,	CompressiveSteel has not Yielded		CompressiveSteel has not Yielded	
$T = A_s f_y$	158	kips	136.5848117	kips
$C_c = .85f_c' \, a \, b_w$	252	kips	252	kips
$C_s = A_s' f_y(\varepsilon_s'/(f_y/E_s))$	142	kips	142	kips
$P = C_s + C_c - T$	236	kips	257	kips
Σ Moments @ Plastic Centroid				
$M = C_c(d/2-a/2) + C_s(d/2 - d') + T(d/2 - d')$	305.31	kip-ft	293.71	kip-ft

Point 6: ε_c = .003 in/in and ε_s = 0 in/in	Tension Steel has No Strain			
Strain of concrete, ε_c	0.003	in/in	0.003	in/in
Strain of steel, ε_s	0	in/in	0	in/in
ε'_s = ε_c (c -d')/c	0.00252	in/in	0.00252	in/in
c= d_s (ε_c/ε_c + ε_s)	15.50	in	15.50	in
a = .85c	13.18	in	13.18	in
Compressive steel stress, f_s' = $E_s\varepsilon_s'$	72,968	psi	72,968	psi
Therefore,	Compressive Steel has Yielded		Compressive Steel has Yielded	
T = A_sf_y	0	kips	0.0	kips
C_c = .85f_c' a b_w	756	kips	755.9	kips
C_s = $A_s'f_y$	158	kips	136.6	kips
P = C_s + C_c - T	914	kips	893	kips
Σ Moments @ Plastic Centroid				
M = C_c(d/2-a/2) + C_s(d/2 - d')+ T(d/2 - d')	237.55	kip-ft	225.95	kip-ft
Point 7: ε_c = .003 in/in and ε_s = .0005 in/in	Very Small Strain in Steel			
Strain of concrete, ε_c	0.003	in/in	0.003	in/in
Strain of steel, ε_s	0.0005	in/in	0.0005	in/in
ε'_s = ε_c (c -d')/c	0.00244	in/in	0.00244	in/in
c= d_s (ε_c/ε_c + ε_s)	13.29	in	13.29	in
a = .85c	11.29	in	11.29	in
Compressive steel stress, f_s' = $E_s\varepsilon_s'$	70,629	psi	70,629	psi
Therefore,	Compressive Steel has Yielded		Compressive Steel has Yielded	
T = A_sf_y(ε_s/(f_y/E_s))	45.82	kips	41.5	kips
C_c = .85f_c' a b_w	648	kips	647.9	kips
C_s = $A_s'f_y$	158	kips	136.6	kips
P = C_s + C_c - T	760	kips	743	kips
Σ Moments @ Plastic Centroid				
M = C_c(d/2-a/2) + C_s(d/2 - d')+ T(d/2 - d')	291.48	kip-ft	277.56	kip-ft

Nominal Strength	M (kip-ft)	P (kips)	M (kip-ft)	P (kips)
Point 1	0	1328.61	0	1285.77
Point 6	237.55	913.92	225.95	892.50
Point 7	291.48	760.11	277.56	742.97
Point 2	377.01	480.03	352.42	488.34
Point 4	350.89	377.96	327.69	377.96
Point 5	305.31	235.87	293.71	257.28
Point 3	212.53	48.83	188.09	46.73

Design Strength

Strength Redundant Factor	M (kip-ft)	P (kips)	M (kip-ft)	P (kips)
Point 1	0	863.59	0	835.75
Point 6	154.4100158	594.05	146.8700849	580.13
Point 7	189.4588448	494.07	180.4144252	482.93
Point 2	245.0596641	312.02	229.0723391	317.42
Point 4	228.0807624	245.67	213.0009006	245.67
Point 5	198.4542566	153.31	190.9143257	167.23
Point 3	138.1439818	31.74	122.2586711	30.37
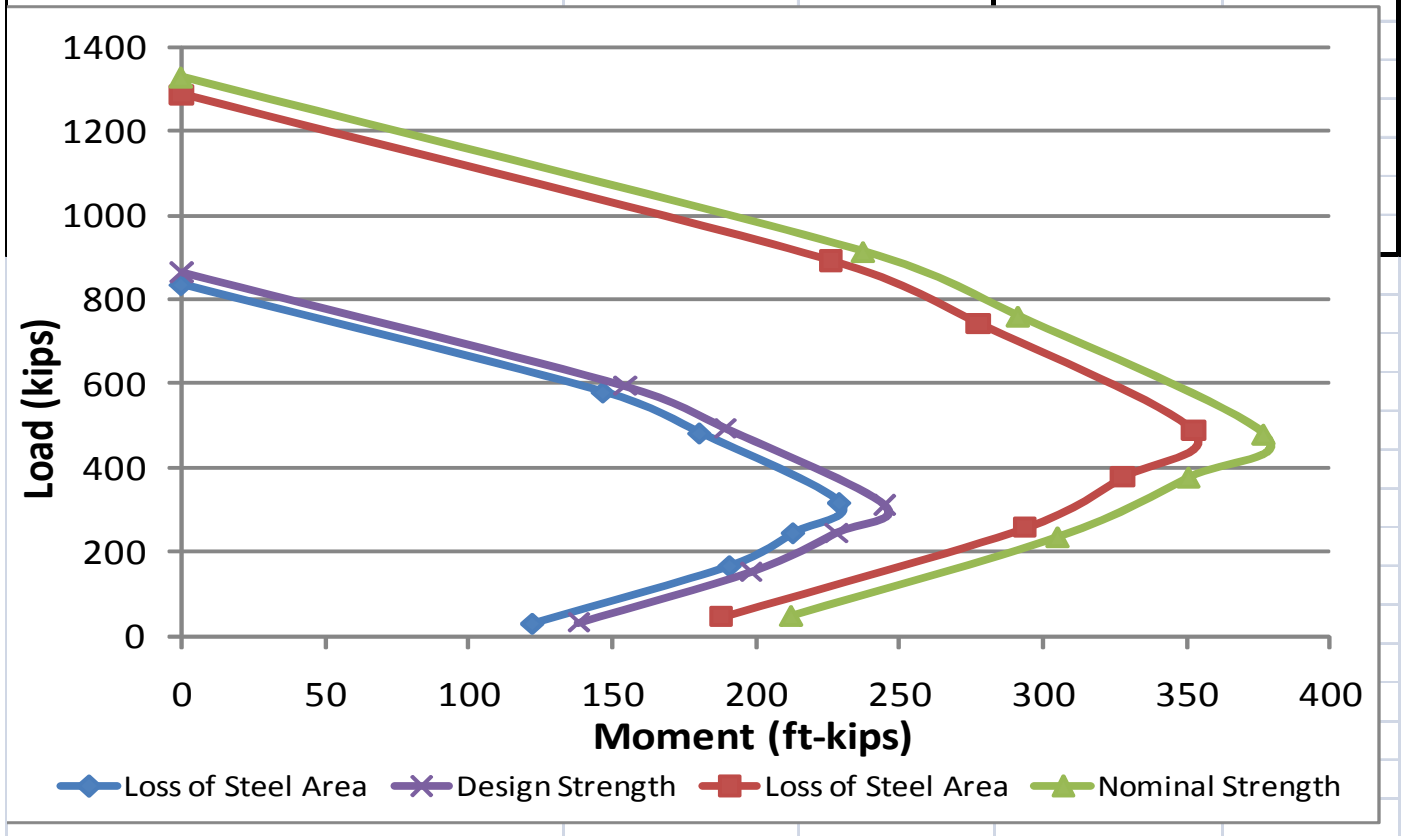
9. Discussion and Conclusions

Chloride induced corrosion of steel reinforcement is the most common cause of deterioration of concrete substructures. With accurate monitoring of the corrosion and repair and rehabilitation procedures at the appropriate times, the service life of structures can be extended. Accurate modeling of steel corrosion in concrete structures is also an important tool that can help the interpretation of the data from corrosion measurement techniques. Although it is difficult to replace non-destructive testing methods, this thesis explores mathematical and empirical models to analyze health condition of reinforced concrete substructures. Empirical models are based on observed correlation between corrosion rate of steel in concrete and different parameters affecting it. These parameters have been researched from authors around the globe and have corresponding results between them. Furthermore, this thesis presents a strength evaluation method for bridge substructures, with a spreadsheet model that outputs the interaction diagram of the original load-moment relationship and the deteriorated load-moment relationship. The results of the thesis investigation are that the corrosion of the reinforcement undoubtedly reduces the ultimate load-carrying capacity and that this capacity loss can be found from proposed models. This strength evaluation procedure is classified with Federal Highway Administration condition ratings. Overall, the thesis and procedure has presented a methodology for improving the understanding of effects of deterioration on the structural performance of concrete columns.

9.1 Summary

1. Service life principles have been described and divided into two periods, the initiation period and the propagation period, which make up the maintenance free life of structure (illustrated in Figure 1.2). The initiation period is defined by the chloride diffusion

process and the propagation period is defined by the corrosion process. Once cracking occurs and a certain crack width is exceeded, then the structure is in need of maintenance.

2. A decision tree in Figure 2.1 is used to illustrate the decision making process in determining a condition rating that is also conducive to the Federal Highway Administration ratings. The "capacity check" portion of the decision making flowchart is schematically represented with a sub-flow chart (Figure 2.2) and illustrates the development of deteriorating factors that contribute to the reduction in strength capacity.

3. Probabilistic performance-based service life is used as the best approach to analyze the initiation period: the time it takes for a certain amount of chloride to reach the reinforcement. This is the best method due to the various parameters involved with the chloride induction process, the concrete compositions and environmental factors.

4. Carbonation can also be a large contribution to the deterioration of concrete substructures. However, the carbonation initiation time is much longer than the initiation time for chlorides, and it can be assumed that repair or rehabilitation actions would take place before complications due to carbonation.

5. An accurate assessment of the surface chloride content and the threshold value is directly proportional with the accuracy of the initiation period of the service life. These two parameters are the main factors behind the time length of the diffusion process. Furthermore, the diffusion model can be precisely assessed when formulated with probabilistic approaches to modeling.

6. Corrosion of the reinforcement occurs at the beginning of the propagation period of the service life model. The empirical corrosion model (equation 6-1) proposed by Liu and Weyers is used to demonstrate the rate of corrosion on the steel reinforcement. While

this model is limited to the parameters that make up the model: chloride content, resistivity, time, and temperature. However, these parameters are also the most important factors in the corrosion process. For example, electrical resistivity of concrete has the highest impact on the rate of the electrical current, and thus equal to the rate of corrosion.
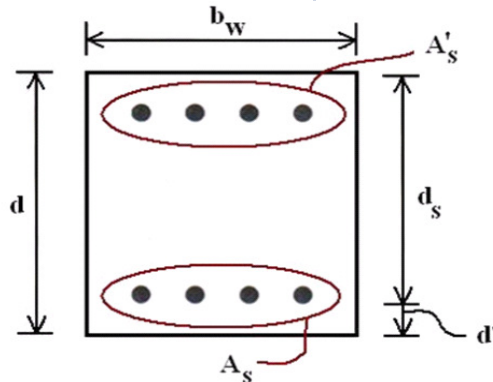
7. Cracking occurs when the rust products from the steel build between the reinforcement and the concrete, thus radiating an outward pressure against the concrete cover. The surface cracking of concrete can be a visual determinate for the present or near future need of repair of concrete piers. These condition ratings are tabulated in Table 7.1.

8. The amount of corrosion is determined based on the corrosion rate, propagation time period, and bar diameter. This percentage is limited to a certain length of the reinforcement is exposed to the environment due to cover loss. However, when there is no length of exposure, the amount of corrosion is assumed to affect the reinforcement on its entire length. Load-Moment diagrams are used to present the strength capacity loss in substructures, by illustrating the loading capacities before and after deterioration.

9.2 Finalized Calculation Process

1. Phil Bamforth's model for diffusion, chloride threshold and surface chlorides has been used to conduct the analysis in the attached appendix. Bamforth's parameters were found to be consistent with other researchers parameter propositions and his experimentation ranged over lengthy time periods.

2. A log-normal distribution was used to model the time for the chloride and carbonation to reach the reinforcement. Assessing the lognormal distribution graphs at the 95% confidence level, the reliability of failure at that time can be accepted with confidence.

3. Bamforth's data is used to solve for the chloride content at the reinforcement and the initiation time for this chloride to reach the reinforcement. Liu and Weyers model is then used to correlate the chloride content with their proposed corrosion rate equation.

4. The amount of corrosion is found from the corrosion rate and thus the reduction of the area and strength of the reinforcement is found. With fundamental concrete design equations, the new capacity of the substructure is analyzed and compared with the original capacity.

Appendix- Sample Spreadsheet

Geometry for Pier		
Design Yield Strength of Reinforcement, f_y (psi)	50,000	
Concrete Compressive Strength, f_c' (psi)	3,750	
Young's Modulus of Steel, E_s (psi)	29,000,000	

depth of pier, d	18	in
width of the pier, b_w	18	in
Cover - Center depth of reinforcement, d'	2.5	
Concrete cover, c	2	in
Number of Bars	4	
Bar Number	8	
Bar Spacing	8	in
Bar Diameter	1	in.
Bar Diameter	25.4	mm.
Bar Area	0.79	in^2
Gross Area of Steel in Compression, A_s	3.16	in^2
Number of Bars	4	
Bar Number	8	
Bar Spacing	8	in
Bar Diameter	1	in.
Bar Diameter	25.4	mm.
Bar Area	0.79	in^2
Gross Area of Steel in Compression, A_s'	3.16	in^2
Number of Bars	8	
depth of steel, d_s	15.5	in.
Gross Area of Concrete & Steel, A_g	324	in^2
Gross Area of Steel, A_{st}	6.32	in^2
Gross Area of Concrete , A_c	317.68	in^2

A_s

A_s'

$A_s + A_s'$

Time in Service	50	years

Mix details & input Data		
Cement content (kg/m^3)	350	
Density(kg/m^2)	2400	
Temperature (Kelvin)	293.15	
W/C ratio	0.45	
Cl threshold level	0.4	(% cement)

Csn(% concrete)	Pc concrete	blnd cmt mix.
Typical	0.36%	0.51%
Upper 90%	0.70%	0.85%
Upper 95%	0.79%	0.94%
Inout for calculation	0.7	

Cement codes	
Portland Cement	pc
pc/pulverised fuel ash	pfa
pc/ground granulated bfs	ggbs
pc/sillica fume	sf
Dce at age of ..Yrs	20

Estimated Dca at 20 years	w/c	Dca at 20 yrs
Pc	0.45	9.41E-13
pfa &ggbs	0.45	2.04E-13
silica fume	0.45	6.25E-13
Input for calculation	0.45	9.41E-13
Reference Time	20	years
$D(t) = D_{ref} (t/t_{ref})^m$ (m^2/s)	7.38811E-13	m^2/s

Age Factor,n	
Portland cement conc	-0.264
Pfa conc	-0.699
ggbs concrete	-0.621
Input for the calculation	-0.264

C_{env} Environmental Coefficient	MPa
Structures Sheltered from Rain	1.00
Structures Exposed to Rain	0.50
Inout for calculation	1

C_{air} Air Content Coefficient	MPa
Non-air-Entrained, (Pc)	1.00
Air-Entrained	0.70
Inout for calculation	1

Binding Agent	a	b
Portland Cement Binder (Type 1)	1800	-1.7
PC +28% Fly Ash (Type 2)	360	-1.2
PC +70% blast furnace slag (Type 2)	360	-1.2
Inout for calculation	1800	-1.7

Table 1 Calculated chloride contents(% cement) with period of exposure and depth

Depth(mm)	Time(yrs)													
	1	2	3	5	10	15	20	30	40	50	60	70	85	100
	Dce(m²/sec)													
	2.0752E-12	1.7282E-12	1.5527E-12	1.3569E-12	1.13E-12	1.0153E-12	9.41E-13	8.4548E-13	7.8364E-13	7.3881E-13	7.0409E-13	6.7601E-13	6.4224E-13	6.1526E-13
	Choloride content (% by wt of cement)													
5	3.18	3.53	3.70	3.88	4.09	4.19	4.25	4.32	4.37	4.40	4.43	4.45	4.47	4.49
10	1.83	2.39	2.69	3.02	3.40	3.59	3.70	3.85	3.95	4.01	4.06	4.10	4.15	4.19
15	0.91	1.49	1.83	2.25	2.76	3.02	3.18	3.40	3.53	3.63	3.70	3.76	3.83	3.89
20	0.39	0.84	1.17	1.60	2.18	2.49	2.70	2.96	3.13	3.26	3.35	3.43	3.52	3.59
25	0.14	0.43	0.70	1.09	1.68	2.02	2.25	2.55	2.76	2.90	3.02	3.11	3.22	3.30
30	0.04	0.20	0.38	0.71	1.25	1.60	1.84	2.18	2.40	2.57	2.69	2.80	2.92	3.03
35	0.01	0.09	0.20	0.44	0.91	1.24	1.49	1.83	2.07	2.25	2.39	2.51	2.64	2.76
40	0.00	0.03	0.09	0.26	0.64	0.95	1.18	1.52	1.77	1.96	2.11	2.23	2.38	2.50
45	0.00	0.01	0.04	0.14	0.44	0.70	0.92	1.25	1.50	1.69	1.84	1.97	2.13	2.26
50	0.00	0.00	0.02	0.08	0.29	0.51	0.70	1.01	1.25	1.44	1.60	1.73	1.89	2.03
55	0.00	0.00	0.01	0.04	0.19	0.37	0.53	0.81	1.04	1.22	1.38	1.51	1.67	1.81
60	0.00	0.00	0.00	0.02	0.12	0.25	0.39	0.64	0.85	1.03	1.18	1.31	1.47	1.61
65	0.00	0.00	0.00	0.01	0.07	0.17	0.28	0.50	0.69	0.86	1.00	1.12	1.29	1.43
70	0.00	0.00	0.00	0.00	0.04	0.11	0.20	0.38	0.55	0.71	0.84	0.96	1.12	1.25
75	0.00	0.00	0.00	0.00	0.02	0.07	0.14	0.29	0.44	0.58	0.70	0.82	0.97	1.10

Chloride Content vs. Time

X-axis: Time, years
Y-axis: Chloride Content, % by wt. of cement

Legend: 5mm, 10mm, 15mm, 20mm, 25mm, 30mm, 35mm, 40mm, 45mm, 50mm, 55mm, 60mm, 65mm, 70mm, 75mm
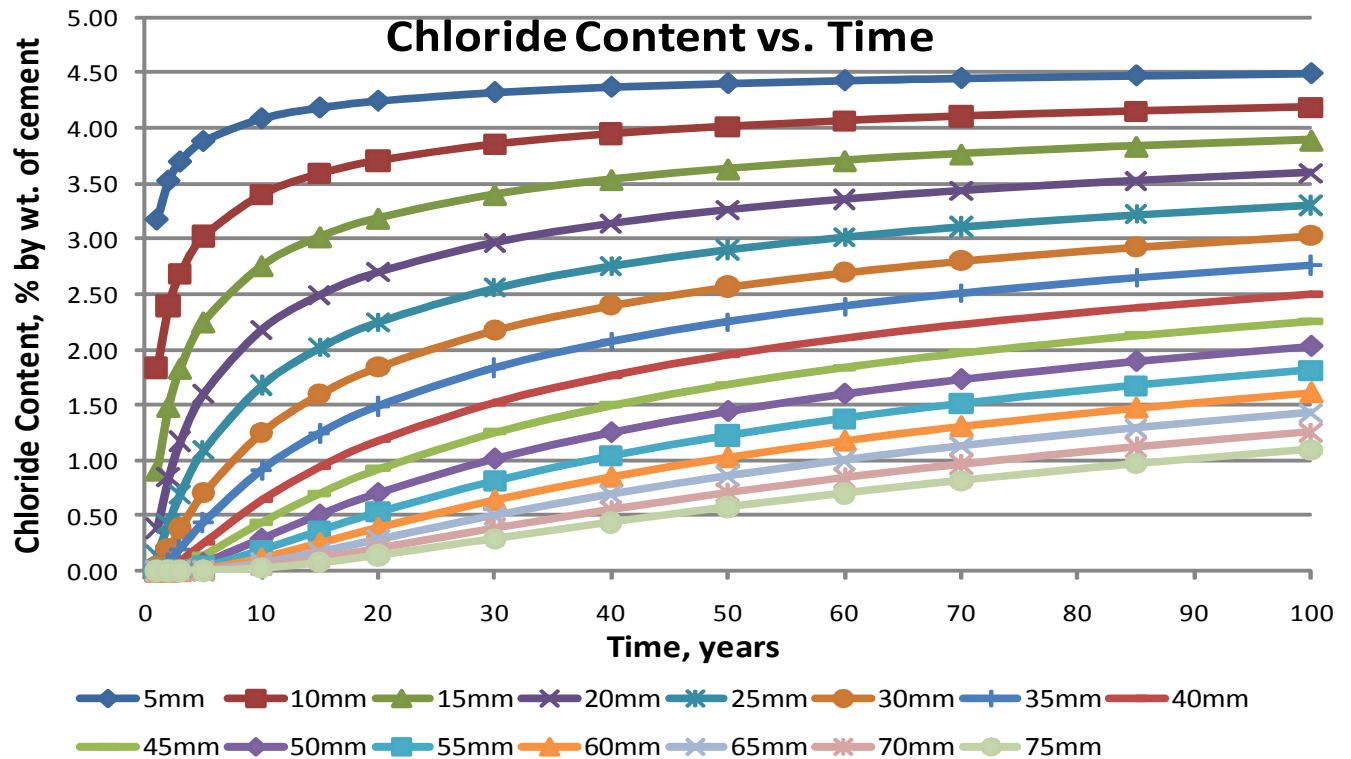
Table 2 Probability of Corrosion Initiation Time from Carbonation

Parameters	Mean	COV
Concrete Cover Depth, mm	50.8	0.2
c_{env} =the environmental coefficient, (MPa)	1	
c_{air} =the coefficient of air content, (MPa)	1	
	a	b
Binding Agent	1800	-1.7
Characteristic Compressive Strength, f_{ck}	30	MPa
μ_x $E[T_{cr}]=(\mu_c/\mu_k)^2 (1+V_c^2)(1+V_k^2)^3$	233.597	
Cov $V[T_{cr}]=sqrt((\{1+V_c^2\}\{1+V_k^2\})^4-1)$	0.701	
σ_x $S[T_{cr}]=E[T_{cr}] \times V[T_{cr}]$	163.668	
$\mu = \ln(E[X]) - .5\ln(1+(S[X]/E[X])^2)$	5.254	
$\sigma = Sqrt(\ln(1+(S[X]/E[X])^2))$	0.632	
$K[T_{cr}]= \exp(E[\ln T_{cr}]-(1.65)S[\ln T_{cr}])$	67.435	
Carbonation Rate Factor, $k_c=c_{env}\,c_{air}\,a(f_{ck}+8)^b$	3.71	0.25
Deterministic Intiation Time, $t_{cr}=(c/k_1)^2$	187.26	years

Carbonation Probability Density

(Y-axis: Failure Probability in a Year; X-axis: Time, years; legend: Carbonation Probability Density)
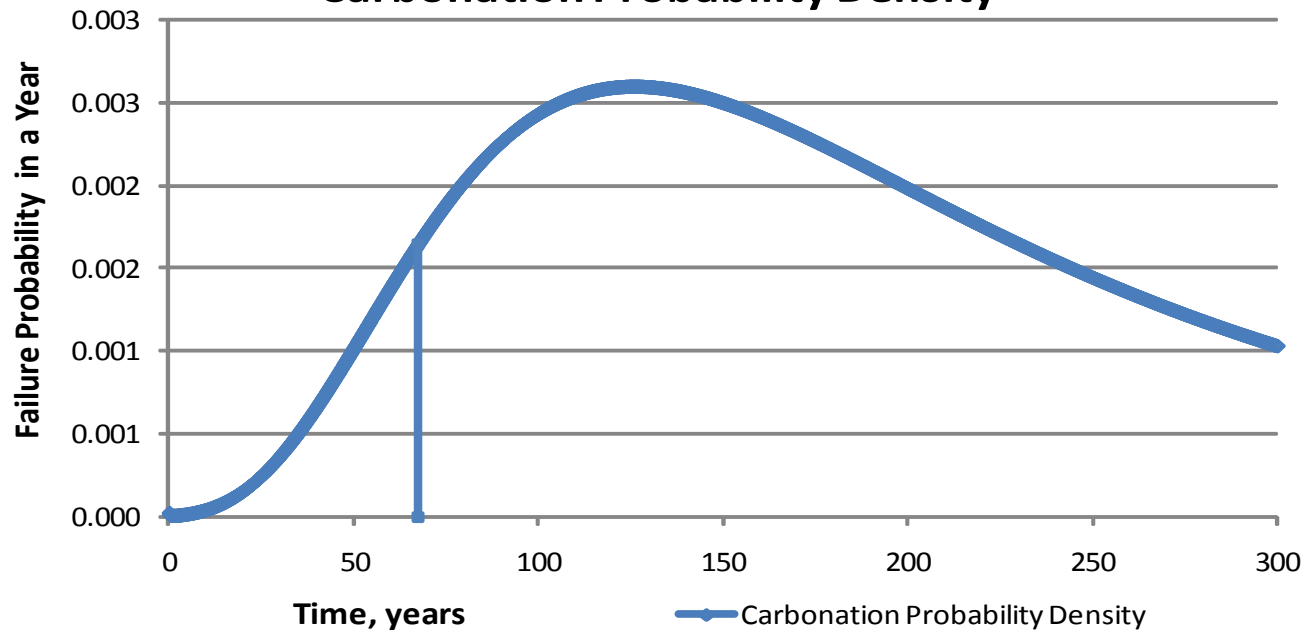
Graphing points	67.5	0.001644905
	67.5	0

Table 3 Probability of Corrosion Initiation Time from Chloride		
Parameters	**Mean**	**COV**
Concrete Cover Depth, mm	50.8	0.2
Surface Chloride Content, %wt of cement	4.8	
Surface Chloride Content, kg/m^3	16.8	
Threshold Chloride Content, %wt of cement	0.4	
Threshold Chloride Content, kg/m^3	1.4	
w/c ratio	0.45	
$D(t) = D_{ref} (t_{ref}/t)m ,(m2/s)$	7.38811E-13	
$E[T_{cr}]=(\mu_c/\mu_k)^2 (1+V_c^2) (1+V_k^2)^3$	23.023	
$V[T_{cr}]=sqrt((\{1+V_c^2\} \{1+V_k^2\})^4-1)$	0.701	
$S[T_{cr}]=E[T_{cr}] \times V[T_{cr}]$	16.131	
$\mu = ln(E[X]) - .5ln(1+(S[X]/E[X])^2)$	3.136	
$\sigma = Sqrt(ln(1+(S[X]/E[X])^2))$	0.632	
$K[T_{cr}]= exp (E[lnT_{cr}]-(1.65)S[lnT_{cr}])$	6.646	
Parameter, k_1	11.82	0.25
Deterministic Intiation Time, $t_{cr} = (c/k_1)^2$	18.46	
$T_j \cong \dfrac{x^2}{4D} \left[erf^{-1}\left(1 - \dfrac{C_{th}}{C_s}\right)\right]^{-2}$		

Chloride Probability Density
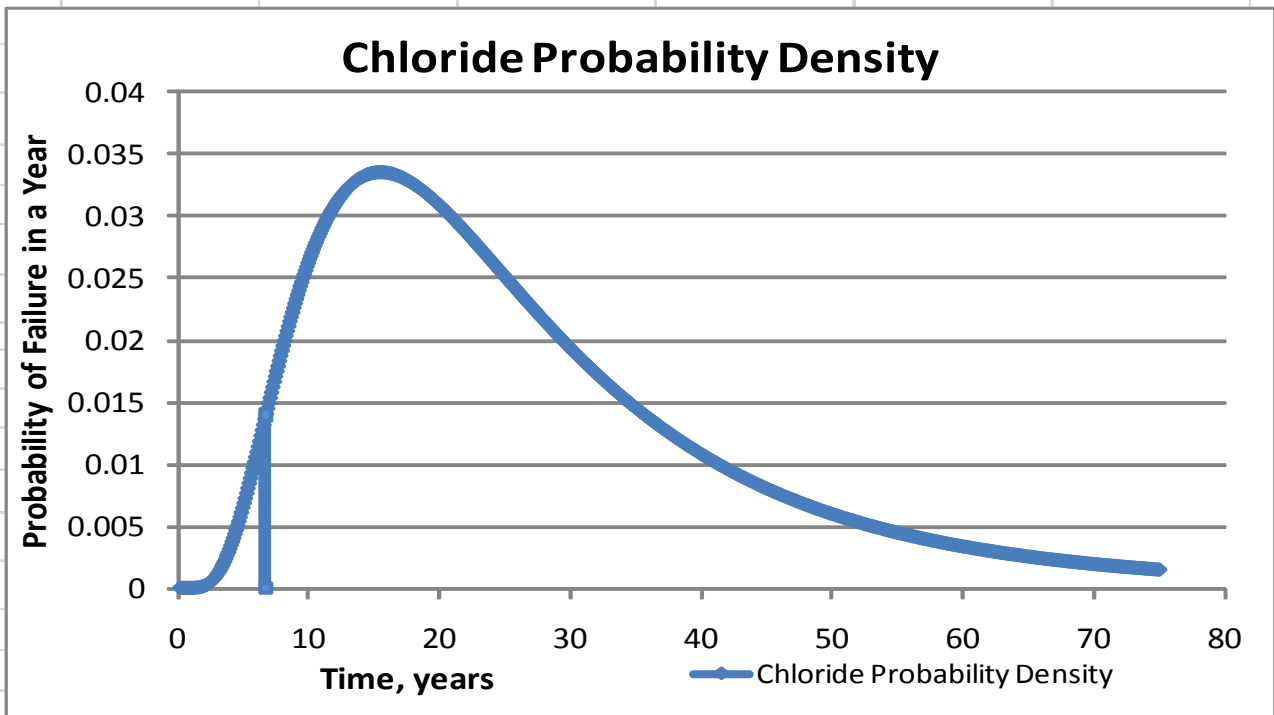
Graphing points	6.7	0.014015284
	6.7	0

Depth (mm)	Table 4 Carbonation Rate Factor													
	Time (yrs)													
	1	2	3	5	10	15	20	30	40	50	60	70	85	100
5	5.00	3.54	2.89	2.24	1.58	1.29	1.12	0.91	0.79	0.71	0.65	0.60	0.54	0.50
10	10.00	7.07	5.77	4.47	3.16	2.58	2.24	1.83	1.58	1.41	1.29	1.20	1.08	1.00
15	15.00	10.61	8.66	6.71	4.74	3.87	3.35	2.74	2.37	2.12	1.94	1.79	1.63	1.50
20	20.00	14.14	11.55	8.94	6.32	5.16	4.47	3.65	3.16	2.83	2.58	2.39	2.17	2.00
25	25.00	17.68	14.43	11.18	7.91	6.45	5.59	4.56	3.95	3.54	3.23	2.99	2.71	2.50
30	30.00	21.21	17.32	13.42	9.49	7.75	6.71	5.48	4.74	4.24	3.87	3.59	3.25	3.00
35	35.00	24.75	20.21	15.65	11.07	9.04	7.83	6.39	5.53	4.95	4.52	4.18	3.80	3.50
40	40.00	28.28	23.09	17.89	12.65	10.33	8.94	7.30	6.32	5.66	5.16	4.78	4.34	4.00
45	45.00	31.82	25.98	20.12	14.23	11.62	10.06	8.22	7.12	6.36	5.81	5.38	4.88	4.50
50	50.00	35.36	28.87	22.36	15.81	12.91	11.18	9.13	7.91	7.07	6.45	5.98	5.42	5.00
55	55.00	38.89	31.75	24.60	17.39	14.20	12.30	10.04	8.70	7.78	7.10	6.57	5.97	5.50
60	60.00	42.43	34.64	26.83	18.97	15.49	13.42	10.95	9.49	8.49	7.75	7.17	6.51	6.00
65	65.00	45.96	37.53	29.07	20.55	16.78	14.53	11.87	10.28	9.19	8.39	7.77	7.05	6.50
70	70.00	49.50	40.41	31.30	22.14	18.07	15.65	12.78	11.07	9.90	9.04	8.37	7.59	7.00
75	75.00	53.03	43.30	33.54	23.72	19.36	16.77	13.69	11.86	10.61	9.68	8.96	8.13	7.50

Carbonation Rate Factor
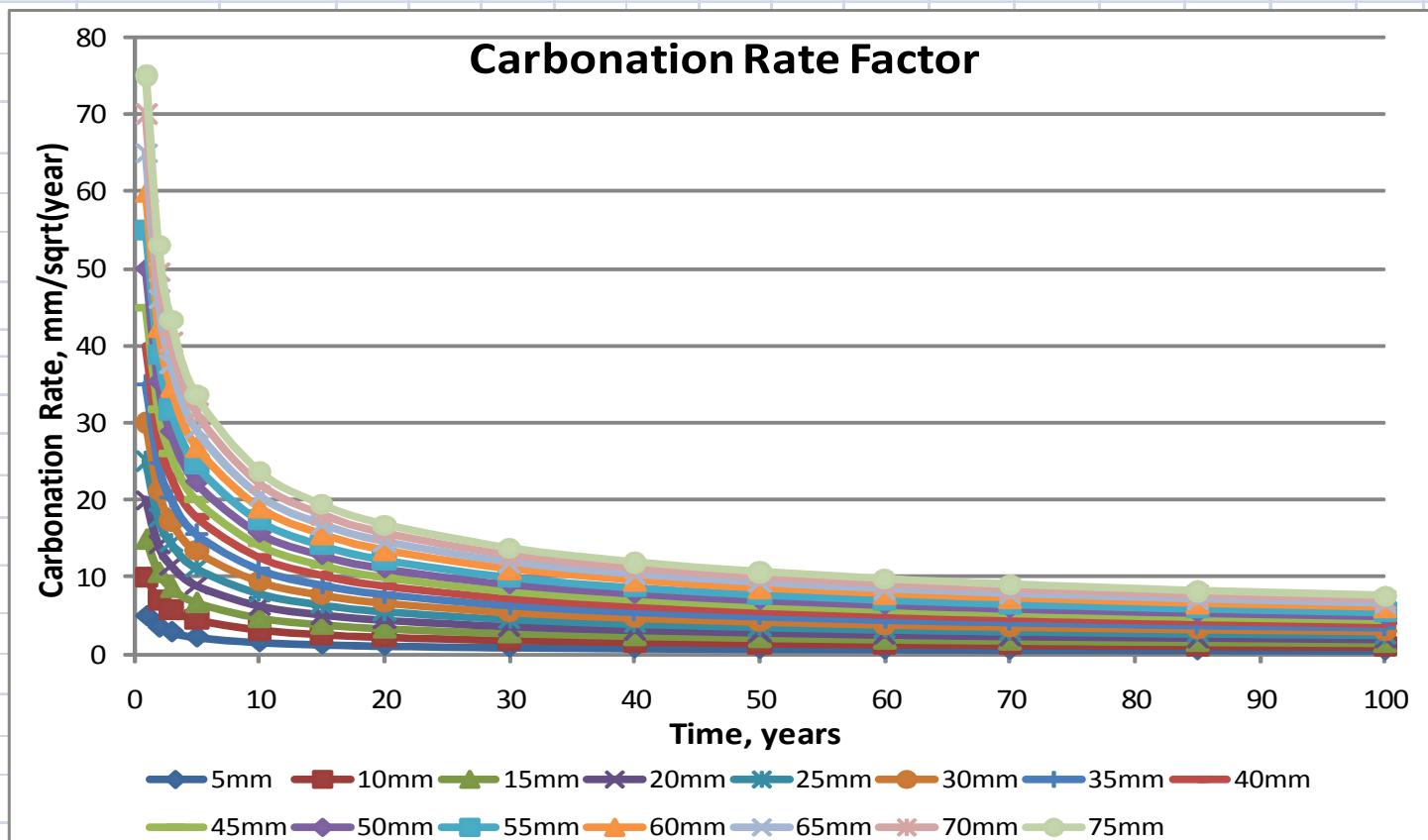
Corrosion Rate		
Probability Time to Activation	6.7	years
Time Elapsed Since Corrosion Initiation	43.30	years
$C(x,t)$ % Wt of Cement	1.41	(equation)
Chloride Content	4.92	kg/m^3
I_{corr}	1.1893	$\mu A/cm^2$
	1.19E-06	A/cm^2
	1.2844	mA/ft^2
	0.0138	mm/year
Percent Amount of Corrosion, Q_{corr} =	9.33%	

Yield or Ultimate Strength		
$f_y = (1.0 - 0.005 Q_{corr}) f_{y0}$	47668.5	psi
f_y / f_{y0}	0.95337	

Tension Steel Difference In Area		
$A_s = (1.0 - 0.01 Q_{corr}) A_{so}$	0.71633	in^2
A_s / A_{so}	0.90674	
Gross Area of Steel in Compression, A_s	2.86530	in^2

A_S

Compression Steel Difference In Area		
$A_s' = (1.0 - 0.01 Q_{corr}) A_{so}$	0.71633	in^2
A_s' / A_{so}	0.90674	
Gross Area of Steel in Compression, A_s'	2.86530	in^2

A_S'

Gross Area of Steel, A_{st}	5.73061	in^2

Difference In Diameter		
New Diameter	0.95502	in
Change in Diameter, ΔD	0.04498	in

Calculation for further reduction of reinforcing steel area due to cracks		
Crack width, Δw	1.496	mm
Change in Diameter, ΔD	1.143	mm
Original Diameter, D	25.4	mm
Cover Depth, c	50.8	mm
$\acute{\alpha} = \rho_{rust}/\rho_{steel}$	2	
Typical values of $\acute{\alpha}$ are 2-4		

$$\Delta w = \Delta D \frac{(\alpha - 1)\pi D}{\left(\frac{D/2}{D/2 + c} + 1\right) c}$$

Depth (mm)	Table 5 Calculation of Corrosion Rate, CR in ($\mu A/cm^2$)													
	Time since start of corrosion (yrs)													
	1	2	3	5	10	15	20	30	40	50	60	70	85	100
5	8.02	6.40	5.66	4.89	4.09	3.72	3.49	3.21	3.04	2.92	2.82	2.75	2.66	2.59
10	5.13	4.67	4.37	3.99	3.53	3.29	3.13	2.93	2.80	2.71	2.63	2.58	2.51	2.45
15	2.89	3.17	3.20	3.15	2.98	2.86	2.77	2.65	2.56	2.50	2.44	2.40	2.35	2.31
20	1.41	1.98	2.21	2.39	2.46	2.45	2.42	2.37	2.33	2.29	2.26	2.23	2.19	2.17
25	0.59	1.14	1.44	1.74	1.99	2.06	2.09	2.10	2.10	2.08	2.07	2.06	2.04	2.02
30	0.22	0.60	0.87	1.21	1.57	1.71	1.78	1.85	1.87	1.89	1.89	1.89	1.89	1.89
35	0.08	0.29	0.50	0.81	1.20	1.39	1.49	1.60	1.66	1.69	1.72	1.73	1.74	1.75
40	0.02	0.13	0.27	0.52	0.90	1.11	1.23	1.38	1.46	1.51	1.55	1.57	1.60	1.62
45	0.01	0.06	0.14	0.32	0.66	0.87	1.00	1.17	1.27	1.34	1.39	1.42	1.46	1.49
50	0.00	0.02	0.07	0.19	0.47	0.66	0.80	0.99	1.10	1.18	1.24	1.28	1.33	1.36
55	0.00	0.01	0.03	0.11	0.32	0.50	0.63	0.82	0.94	1.03	1.09	1.14	1.20	1.24
60	0.00	0.00	0.01	0.06	0.22	0.37	0.49	0.67	0.80	0.89	0.96	1.02	1.08	1.13
65	0.00	0.00	0.01	0.03	0.14	0.27	0.38	0.55	0.67	0.77	0.84	0.90	0.97	1.02
70	0.00	0.00	0.00	0.02	0.09	0.19	0.28	0.44	0.56	0.65	0.73	0.79	0.86	0.92
75	0.00	0.00	0.00	0.01	0.06	0.13	0.21	0.35	0.46	0.55	0.63	0.69	0.76	0.82

Corrosion Rate vs. Time
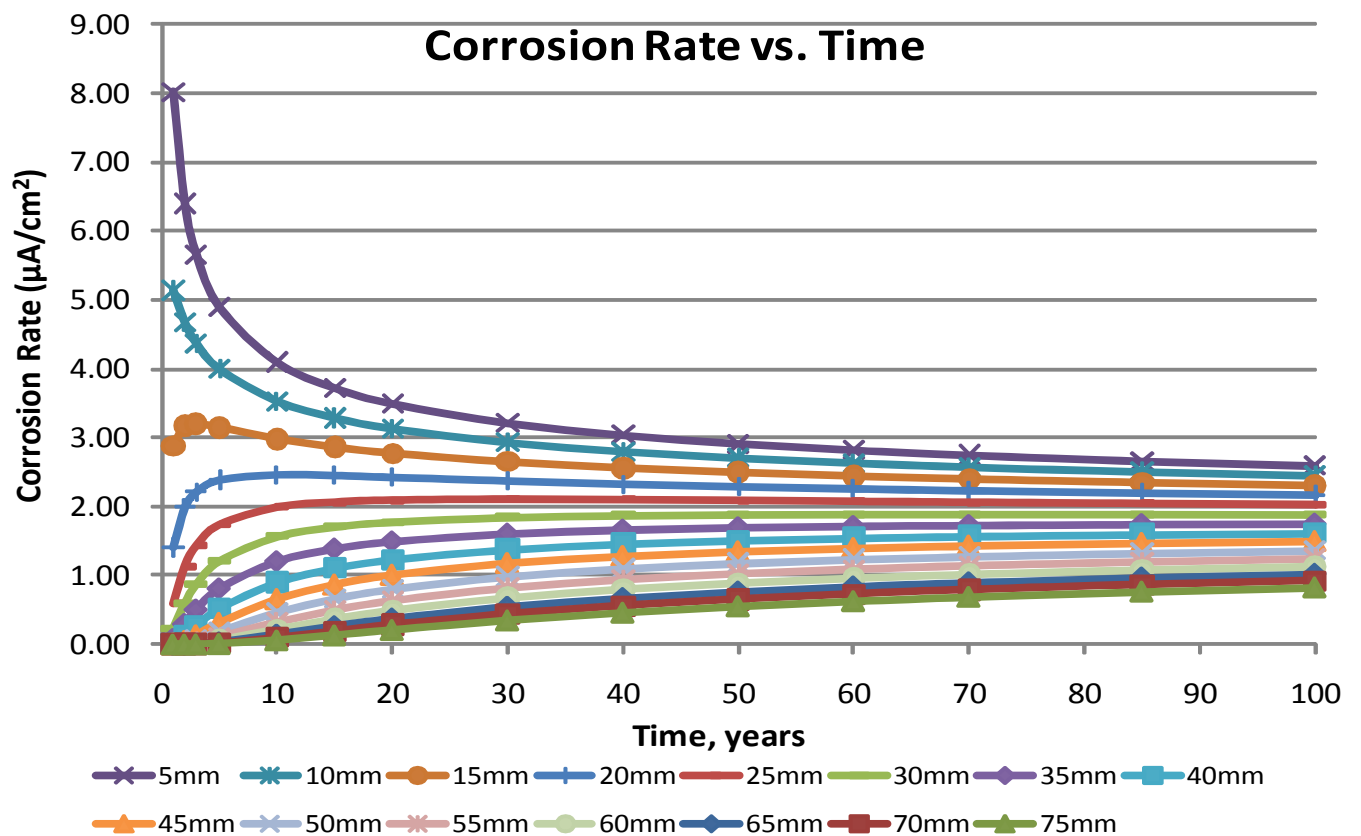
Depth (mm)	Table 6 Calculation Q_{corr} Amount of Corrosion													
	Time since start of corrosion (yrs)													
	1	2	3	5	10	15	20	30	40	50	60	70	85	100
5	1.48%	2.37%	3.14%	4.53%	7.58%	10.3%	12.9%	17.8%	22.5%	27.0%	31.3%	35.6%	41.8%	48.0%
10	0.95%	1.73%	2.43%	3.70%	6.53%	9.1%	11.6%	16.3%	20.7%	25.0%	29.2%	33.4%	39.4%	45.3%
15	0.53%	1.17%	1.78%	2.91%	5.51%	7.9%	10.3%	14.7%	19.0%	23.1%	27.1%	31.1%	37.0%	42.7%
20	0.26%	0.73%	1.23%	2.21%	4.56%	6.8%	9.0%	13.2%	17.2%	21.2%	25.0%	28.9%	34.5%	40.1%
25	0.11%	0.42%	0.80%	1.61%	3.68%	5.7%	7.7%	11.7%	15.5%	19.3%	23.0%	26.7%	32.1%	37.5%
30	0.04%	0.22%	0.49%	1.12%	2.90%	4.7%	6.6%	10.2%	13.9%	17.4%	21.0%	24.5%	29.7%	34.9%
35	0.01%	0.11%	0.28%	0.75%	2.23%	3.9%	5.5%	8.9%	12.3%	15.7%	19.0%	22.4%	27.4%	32.4%
40	0.00%	0.05%	0.15%	0.48%	1.67%	3.1%	4.6%	7.7%	10.8%	14.0%	17.2%	20.4%	25.1%	29.9%
45	0.00%	0.02%	0.08%	0.29%	1.21%	2.4%	3.7%	6.5%	9.4%	12.4%	15.4%	18.4%	23.0%	27.5%
50	0.00%	0.01%	0.04%	0.17%	0.86%	1.8%	3.0%	5.5%	8.1%	10.9%	13.7%	16.6%	20.9%	25.2%
55	0.00%	0.00%	0.02%	0.10%	0.60%	1.4%	2.3%	4.6%	7.0%	9.5%	12.1%	14.8%	18.9%	23.0%
60	0.00%	0.00%	0.01%	0.05%	0.40%	1.0%	1.8%	3.7%	5.9%	8.2%	10.7%	13.2%	17.0%	20.9%
65	0.00%	0.00%	0.00%	0.03%	0.27%	0.7%	1.4%	3.0%	5.0%	7.1%	9.3%	11.6%	15.2%	18.9%
70	0.00%	0.00%	0.00%	0.02%	0.17%	0.5%	1.0%	2.4%	4.1%	6.0%	8.1%	10.2%	13.5%	17.0%
75	0.00%	0.00%	0.00%	0.01%	0.11%	0.4%	0.8%	1.9%	3.4%	5.1%	6.9%	8.9%	12.0%	15.2%

Amount of Corrosion vs. Time

Legend: 5mm, 10mm, 15mm, 20mm, 25mm, 30mm, 35mm, 40mm, 45mm, 50mm, 55mm, 60mm, 65mm, 70mm, 75mm
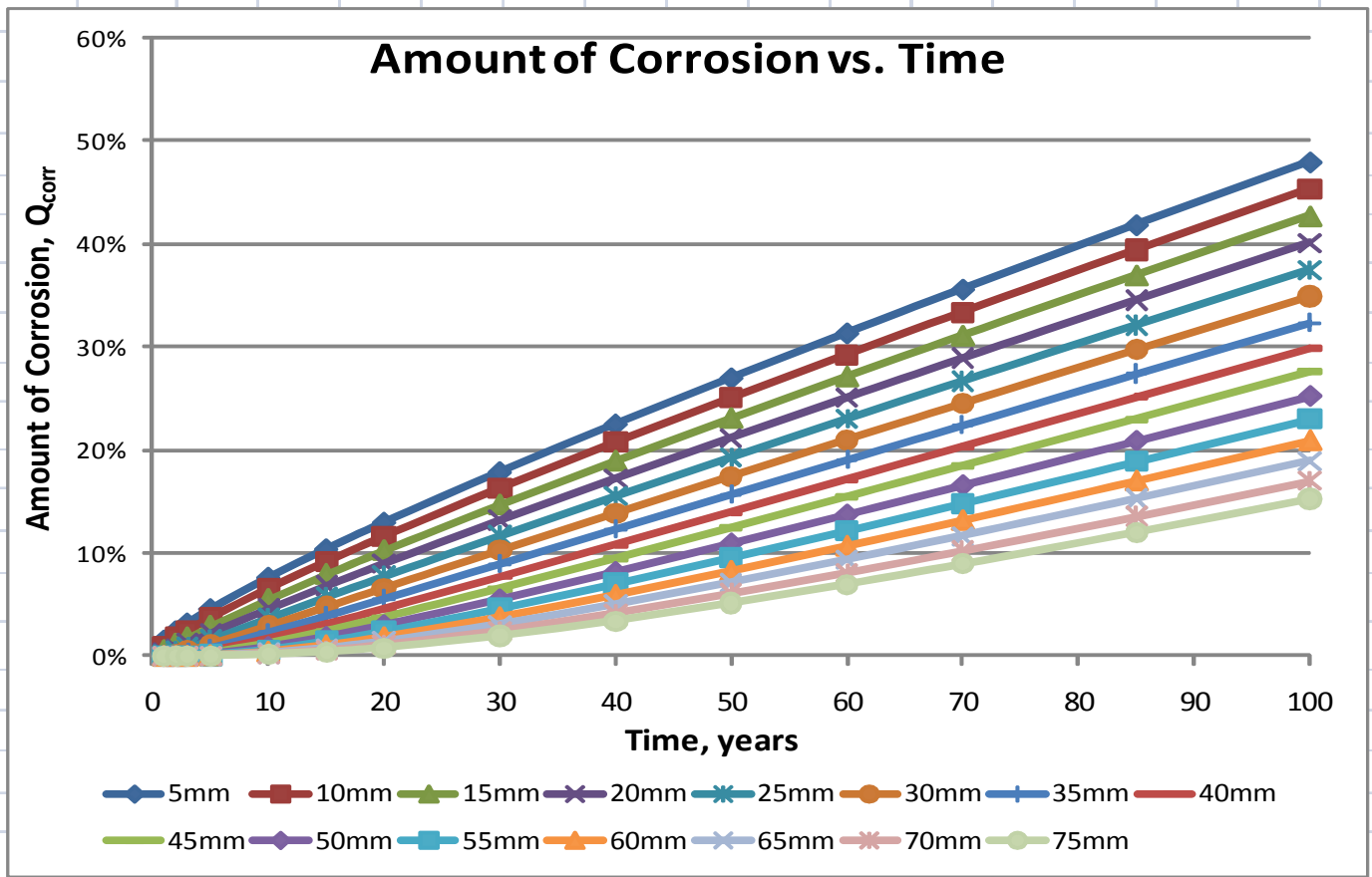
Bibliography

Al-Wazeer, Adel Abdel-Rahman. Risk-Based Bridge Maintenance Strategies. Department of Civil and Environmental Engineering. Doctor of Philosophy 2007.

Arup, H. (1983). "The mechanisms of the protection of steel by concrete", in "Corrosion of Reinforcement in Concrete Construction" (Crane, A. P., Ed.), Ellis Horwood Limited, UK, Chapter 10, pp 151-157. **Found in:** Markeset, Gro and Myrdal, Roar. (2008). Modelling of reinforcement corrosion in concrete – State of the art. Sintef Building and Infrastructure. COIN Project report 7-2008.

ASTM Standard C42, 2003. ASTM C42 / C42M - 10 Standard Test Method for Obtaining and Testing Drilled Cores and Sawed Beams of Concrete. ASTM International, West Conshohocken, PA, 2003, DOI: 10.1520/C0042M-10, www.astm.org.

Ayyub, Bilal M. (2003). "Risk Analysis in Engineering and Economics." Chapman & Hall/CRC.

Bamforth, P.B., (1999). "Options for Reducing the Risk of Reinforcment Corrosion in R.C. Structures and their Incorporation Into the Design Process." Anti-Corrosion Methods and Materials. Voluve 46. Number 4. 1999. pp 268-275

Bamforth, P.B., (1998). "Spreadsheet model for reinforcement corrosion in structures exposed to chlorides." **Found In:** Gjorv, K. Sakai and N. Banthia Editors, *Concrete uncer Severe Conditoins 2* E& FN Spon, London (1998), pp 64-75.

Bamforth, P.B., (1997). "Corrosion of reinforcement in concrete caused by wetting and drying cycles in chloride- containing environments – Results obtained from RC blocks exposed for 9 years adjacent to bridge piers on the A19 near Middlesborough", Taywood Engineering Ltd report PBB/BM/1746.

Bertolini, Luc, Bernhard Elsener, Pietro Pedeferri, and Rob Polder. (2004). Corrosion of Steel in Concrete. Wiley-VCH. Ch. 6. pp. 91-108.

Berver, Emily W.; Jirsa, James. O.; Fowler, David. W.; Wheat, Harovel. G. Moonitoring Corrosion Activity in Chloride contaminated Concrete Wrapped with Fiber Reinforced Plastics. The University of Texas Austin.

Chen, Doug; and Mahadevan, Sankaran. (2007). Chloride-induced reinforcement corrosion and concrete cracking simulation. Elsevier Ltd. Cement and Concrete Composites. 29 April 2007.

Cement Concrete and Aggregates Australia. (2009). Chloride Resistance of Concrete. www.ccaa.com.au. June 2009.

CTI Consultants. (2004). Chlorides in Concrete. CTI Technicla Note C2. CTI Consultants PTY LTD. January 2004.

Dy, Y.G.; Clark, L.A.; and Chan, A.H.C. (2005a). "Effect of corrosion on ductility of reinforcing bars." Mag. Concrete Research. Vol.57, No. 7, pp 407-419.

Du, Y. G., Clark, L.A., and Chan, A. H. C. (2005b). "Residual Capacity of Corroded Reinforcing Bars." Mag. Concrete Res., Vol. 57, No. 3, pp. 135-147.

Elsener, B. (2001). Half-cell potential mapping to assess repair work on RC structures. Construction and Building Materials, Elsevier Science Ltd.

Frangopol, Dan M.; Bruhwiler, Eugen; Faber, Michael H.; Adey, Bryan. (2004). Life-Cycle Performance of Deteriorating Structures Assessment, Design and Management. ASCE.

Frederiksen, Nilsson, Sandberg, Poulsen, Tang and Andersen, (1997) HETEK a System of Estimation of Chlooride Ingress into Concrete, Theoretical Background. Report No. 83:1997. The Danish Road Directorage. Copenhagen, Denmark 1997. Found in: Poulsen, Ervin and Mejlbro, Leif. Diffusion of Chloride in Concrete: Theory and Application. Taylor and Francis Group (2006).

Glass, G.K. and Buenfeld, N.R. (1997). The Presentation of the Chloride Threshold Level for Corrosion of Steel in Concrete. Elsevier Science Ltd. Vol 38. No.5 pp 1001-1013

Gu, Ping and J.J. Beaudoin. (1998). Obtaining Effective Half-Cell Potential Measurements in Reinforced Concrete Structures. National Research Council Canada.

Howlader, Sanjeev K. (2008). Evaluation of Concrete Substructure Elements to Assist in Decision Making of Removal vs. Retainment/Restoration. Graduate School of the University of Maryland.

Lounis, Zoubir and Lyne Daigle. (2008). Reliability-Based Decision Support Tool for Life Cycle Design and Management of Highway Bridge Decks. Institute for Research in Construction. National Research Council Canada. Annual Conference of the Transportation Association of Canada.

Liu, Youping. (1996). Modeling the Time-to-corrosion Cracking of the Cover Concrete in Chloride Contaminated Reinforced Concrete Structures. Virginia Polytechnic Institute and State University, Blacksburg, VA.

Maaddawy, Tamer EL; and Soudki, Khaled. (2007). A model for prediction of time fro mcorrosion initiation to corrosion cracking. Elsevier Ltd. Cement and Concrete Composites. 04 January 2007.

Markeset, Gro and Myrdal, Roar. (2008). Modelling of reinforcement corrosion in concrete – State of the art. Sintef Building and Infrastructure. COIN Project report 7-2008.

Martin-Perez, Beatriz. (1999). Service Life Modelling of R.C. Highway Structures Exposed to Chlorides. National Library of Canada. University of Toronto: Department of Civil Engineering.

Parameswaran, Lakshmy; Kumar, Ram; and Sahu, G.K. (2008). Effect of Carbonation on Concrete Bridge Service Life. ASCE Journal of Bridge Engineering January/February.

Pouslen, Ervin and Mejlbro, Leif. (2006). Diffusion of Chloride in Concrete: Theory and Application. Taylor and Francis Group.

Sarja, A. and Vesikari, E. (1996). Durability Design of Concrete Structures. Report of RILEM Technical Committee 130-CSL. Chapman & Hall: 4-17

Shim, Hyung-seop. (2002). Corner effect on Chloride Ion Diffusion in Rectangular Concrete Media. KSCE Journal of Civil Engineering. Vol. 6 No. 1. March 2002.

Sohanghpurwala, Ali Akbar. (2006), NCHRP National Cooperative Highway Research Program. Manual on Service Life of Corrosion-Damaged Reinforced Concrete Bridge Superstructure Elements. Transportation Research Board of the National Academies.

Stewart, Mark G. and David V Rosowsky. (1998) Structural Safety and Serviceability of Concrete Bridges Subject to Corrosion. ASCE Libraryr. Journal of Infrastructure systems, December, 1998.

Shim, Hyung-seop. (2002). Corner Effect on Chloride Ion Diffusion in Rectangular Concrete Media. KSCE Journal of Civil Engineering. March 2001.

Shim, Hyung-seop. (2001). Interpretation of Field Tests in Condition Assessment of Bridge Element. KSCE Journal of Civil Engineering. March 2001.

Song, Ha-Won, Hyun-Bo Shim, Aruz Petcherdchoo Sun-Kyu Park. (2008). Service life prediction of repaired concrete structures under chloride environment using finite difference method. Cement and Concrete Composites. Elsevier Journal. December 3, 2008.

Stewart, Mark G. and Rosowsky, David. (1998). "Structural Safety and Serviceability of Concrete Bridges Subject to Corrosion. Journal of Infrasturcutre Systems. Decemeber 1998: 146-154.

Tapan, Mucip, and Aboutaha, Riyad S. (2008). Strength Evaluation of Deteriorated RC Bridge Columns. Journal of Bridge Engineering ASCE May/June 2008.

Thoft-Christensen, Palle., (2004). Corrosion and Cracking of Reinforced Concrete. Editors: Dan M. Frangopol. Eugen Bruhwiler, Michael H. Faber, Bryan Adey. Life-cycle Performance of Deteriorating Structures; Assessment, Design, and Management. American Society of Civil Engineers.2004.

Vu, Kim Anh T., & Stewart, Mark G. (2000). "Structural reliability of concrete bridges including Improved chloride-induced corrosion models." Structural Safety 22.4 (2000): 313-333

Weyers, R. E., Fitch, M. G., Larsen, E. P., Al-Qadi, I. L., Chamberlain, W. P., and Hoffman, P. C. 1994. Concrete Bridge Protection and Rehabilitation: Chemical and Physical Techniques - Service Life Estimates. SHRP-S-668, Strategic Highway Research Program, National Research Council. **Found in:** Lounis, Zoubir and Lyne Daigle. (2008). Reliability-Based Decision Support Tool for Life Cycle Design and Management of Highway Bridge Decks. Institute for Research in Construction. National Research Council Canada. Annual Conference of the Transportation Association of Canada.